The air pollution benefits of low severity fire

Iván Higuera-Mendieta*[1,2] and Marshall Burke[2,3,4]

[1] *Department of Earth System Science, Stanford University*
[2] *Doerr School of Sustainability, Stanford University*
[3] *National Bureau of Economic Research (NBER)*
[4] *Center on Food Security and the Environment, Stanford University*

December 8, 2025

Abstract

Larger and more frequent wildfire events in Western North America in recent years have resulted in extensive human and environmental damage, and are reversing decades of air quality improvements. Fuels treatments, including the use of prescribed fire, can reduce the extent and severity of future wildfires, but air quality trade-offs resulting from application of these treatments – more initial smoke from prescribed burning in hopes of less smoke from future wildfire – remain poorly quantified. Using two decades of high-resolution satellite-derived measurements of fire severity and fire smoke particulate matter across California, we assess the causal effect of low-severity wildfire – a proxy for prescribed burning – on subsequent wildfire activity and air quality, with particular attention to whether low-severity fire also reduces subsequent fire risk in surrounding unburned areas. We find that locations "treated" with low severity fire see an immediate 92% reduction in the probability of very high severity wildfires in the same location, with detectable reductions in high-severity fire risk lasting up to a decade and detectable up to 5 km from the treated locations. We estimate that the future benefits of low-severity fuel "treatments", in terms of reduced smoke from severe fires, substantially outweigh the costs of the smoke produced in the initial treatment fires, with benefit-cost ratios that exceed six after a decade even under a high discount rate ($> 6\%$). Benefits and costs rise roughly linearly with the amount of area treated. We estimate that a policy of 500 thousand acres of low-severity treatments per year in CA, sustained for a decade, would have reduced cumulative smoke $PM_{2.5}$ concentrations by roughly 10% by the end of the period. These results suggest that substantial expansion of limited current prescribed burned acreage could have meaningful air quality benefits.

The paper is a non-peer reviewed preprint submitted to EarthArXiv. It has been submitted for publication in a peer reviewed journal, but has yet to be formally accepted for publication.

*Corresponding author: Iván Higuera-Mendieta (ihigueme@stanford.edu). We thank seminar participants at Stanford, the World Forestry Center, and Makoto Kelp, Minghao Qiu, Michael Wara, Nicholas Enstice, and Apoorva Lal for helpful feedback. We thank the Stanford Research Computing Center for providing computational resources and support, and thank the Keck Foundation and the Stanford Data Science Fellowship for funding.

1 Introduction

A policy of fire suppression has dominated land management in the Western United States for a century [50], giving rise to the growth of forests' understory fuels and helping to increase the occurrence of larger and more extreme wildfires [3, 31]. This "fire paradox" [23], where putting out fires today can create larger fires in the future, is being amplified by a warming climate, which has dried these fuels and further increased the likelihood of extreme wildfires [1]. Future warming is likely to further exacerbate this activity, perhaps dramatically, even within the next few decades [40, 33].

Ongoing increases in the number and severity of wildfires has had a demonstrable negative effect on a range of health and related outcomes, in large part through the smoke that these fires produce [20, 52, 9, 4, 19, 7]. Growing smoke exposures are relevant for populations in the immediacy of active wildfire areas, but also to those much further away, as experienced in 2023 at a large scale in the Eastern United States from smoke from distant Canadian fires. Emissions and resulting air pollution from wildfires are already undoing decades of progress in improving air quality in the United States [10], and could potentially curtail the ability to meet greenhouse gas emissions goals [25].

Prescribed burning, or the purposeful use of low severity fire to reduce fuel loads, is a central proposed strategy for reducing the likelihood of severe wildfires and the impacts that they cause [37, 38]. A large literature has shown that such burning can have extensive benefits by mitigating future fire spread [6], intensity and severity [55, 34, 14], and tree mortality [42]. However, prescribed burning also entails costs, including the associated particulate matter ($PM_{2.5}$) from burning [22, 32]. While prescribed fires and low-severity fires are thought to have less attributable smoke $PM_{2.5}$ than large wildfires [54], precisely quantifying the air quality impacts and resulting population exposures and health impacts of these fuel treatments remains challenging for at least two reasons. First, limited acreage in the Western US is currently treated with prescribed burning (44,000 acres/year average since 2000, as compared to 866,145 acres/year average of wildfire), which makes it difficult to comprehensively understand the benefits in terms of reduced future fire risk for both treated areas and nearby untreated areas, and how these benefits differ by land type and the underlying likelihood of extreme fire. Second, the lack of adequate air quality monitoring systems throughout much of the West has made understanding emissions and pollution impacts difficult [24, 28]. Evidence from the more densely populated Southeastern US, where yearly 11 million acres (13 times the total area of Western US prescribed burning) are treated on a yearly average, suggests that prescribed burning can substantially increase both air pollution and health impacts [32], with an estimated three-fold increase in the pulmonary disease burden in areas frequently exposed to treatments [2, 22]. Absent comprehensive information on how the application of prescribed fire alters future fire risk, emissions, and air pollution in Western landscapes, land managers and policy makers have limited guidance on how to resolve a new paradox: does it make sense to emit today in hopes of larger emissions reductions in the future?

Here, we comprehensively quantify this trade-off by constructing satellite-derived severity estimates for the majority of wildfires in California from 2000 to 2021 (98.9% of all wildfire events reported by the Monitoring Trends in Burning Severity (MTBS) project), and combining these with fire-specific estimates of resulting smoke $PM_{2.5}$ emissions from 2006 to 2020 using data from [12] and [53]. Satellite data provides high resolution insight into variation in burn severity within and across fires (Fig 1). Given the limited use of prescribed fire in the historical record, we proxy prescribed fire with areas in existing wildfires that burned at low severity, a commonly used approach in the literature [55, 45]. Importantly, satellite data indicate that low-severity wildfire and observed prescribed fires are comparable in terms of burn severity (Fig S10), making the former a reasonable proxy for the latter. Similar to the goal of prescribed fire, low-severity fire limits fuel build up and promotes fire-resistant tree species which encourages future low-severity fire [49,

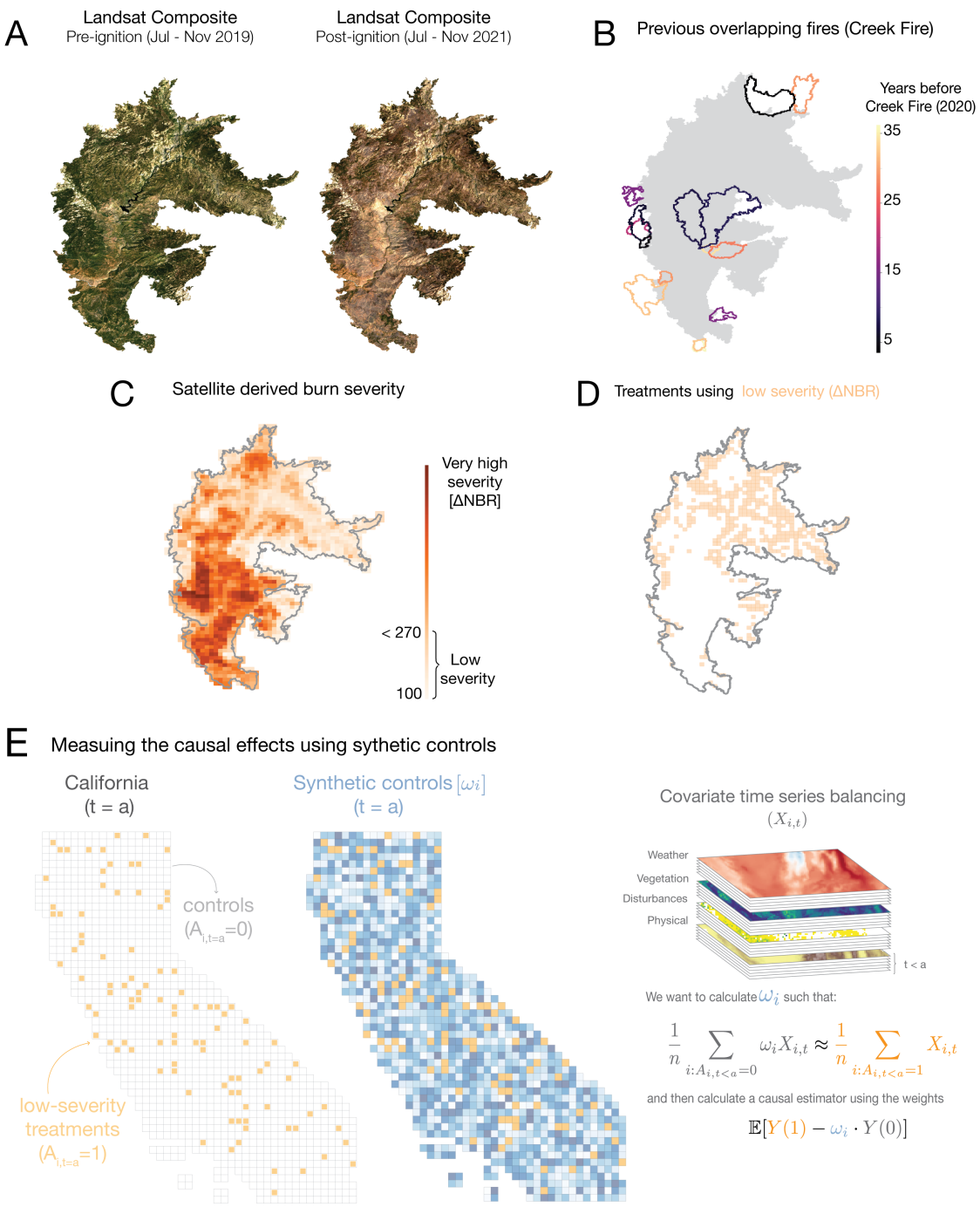

Figure 1: Capturing low-severity fire exposure with satellite imagery and exploiting the spatial distribution and timing of wildfires. **a.** Landsat mean composites for before and after the 2020 Creek Fire, one of the 1,047 fires in our dataset. The pre-fire and post-fire composites are calculated using images for the Western fire season one year before and after the event, respectively. **b.** Previous large wildfires overlapping and surrounding the Creek Fire over the previous three decades. **c-d.** Estimated fire severity (using the Differenced Normalized Burn Ratio ΔNBR) for the Creek Fire, and selection of 1 km^2 pixels "treated" with low-severity fire (defined as $100 \leq \Delta NBR < 270$). **e.** Pictorial depiction of our synthetic control method, in which we use covariate balancing to find a weighted set of untreated pixels that are most similar to our treated pixels prior to treatment period *a*. [See Methods SI]

48]. Our focus on satellite-derived measures of fire severity, rather than fire intensity as in related past work [55], is meant to better capture accumulated change in vegetation during fire, and is much better correlated with estimated fire emissions (Fig S17).

To estimate the impact of low-severity fire on future fire risk, we use a synthetic control approach [56] to match each of 82,592 "treated" low-severity fire 1 km^2 pixels to untreated pixels that are similar to treated units on observable characteristics that are strongly predictive of fire risk prior to treatment; these variables include no burning in the 8 years prior to treatment, and balance on cumulative fire severity prior to 8 years up to the beginning of the satellite record, monthly weather, vegetation characteristics and disturbances, and physical covariates (i.e. slope and elevation) (Fig 1E and Supplementary Materials). As shown by [55], who applied a similar approach to understand the effects of fire-intensity, this covariate time series balancing approach offers a robust method for using untreated matched pixels as a counterfactual for what would have happened in treated pixels absent treatment (Methods SI and Fig S2).

Using this synthetic control estimation, we then track the occurrence of future fire activity in subsequent years across treated pixels and matched controls (Methods SI and Fig 1E), allowing us to estimate the impact of low-severity fire on the risk and severity of future fires for more than a decade following the initial treatment. Given that different vegetation types can have different responses to treatment, we separately estimate the effect of low-severity exposure for different land cover classes.

The effect of past fires on future fire risk is not necessarily limited to locations that directly burned. A host of evidence suggests that wildfires can have a limiting effect on the prevalence and severity of future fires in surrounding non-burned areas [34, 35, 46], in part because because past burns can act as temporary fuel breaks [51, 35], reducing fuel availability and creating vegetation patterns that reduce fire spread probability [46]. Such spillover or "shadow" effects of treatments on nearby untreated areas are a potentially important benefit of fuels treatments, but have not been quantified at large scale. To quantify these potential spillovers, we use the same synthetic control approach but redefine "treated" pixels as those unburned pixels within a given radius of pixels that burned at low severity. (Methods SI and Figure 3). These pixels are again matched with unburned pixels further from a fire, and we track the occurrence of future fire activity across burn-adjacent pixels and matched controls. In this spillover analysis, we restrict the estimation sample to fires that did not burn in close proximity to urban areas, as fire spread in Wildland-Urban Interface (WUI) contexts could be limited by other factors (e.g. roads, or suppression near inhabited areas).

Finally, to understand the costs and benefits of expanded prescribed burn activity on air quality, we combine these causal estimates of the impact of low severity fire on future fire risk with new empirical estimates of the relationship between observed fire severity and fire-specific attributable smoke $PM_{2.5}$ emissions, the latter estimated from previously published data [53]. We then simulate the impact of different prescribed burn policies that treat increasing numbers of acres of conifer forests in California per year with low-severity fire, including ambitious existing policy proposals in the state to burn 1 million acres per year [11]. This calculation depends on both the smoke generated by low-severity treatments as well as the resulting change in subsequent wildfire smoke that occurs due to lessened likelihood of high-severity fire, which in turn depends critically on the likelihood that any treated pixel is exposed to subsequent wildfire, which is low in any given year (Methods SI). Applying our policy simulation to observed fire activity since 2010, we compare the observed amount of fire activity and smoke that occurred since 2010 in California with what our estimates imply would have occurred had a given amount of low-severity treatments occurred annually since 2010, tracking benefits in both treated and nearby (2 km) untreated pixels as informed by our causal estimates (Figs 4, S8). We then calculate the ratio of discounted benefits and costs that would face a policymaker embarking on this policy in 2010, under a range of discount rates.

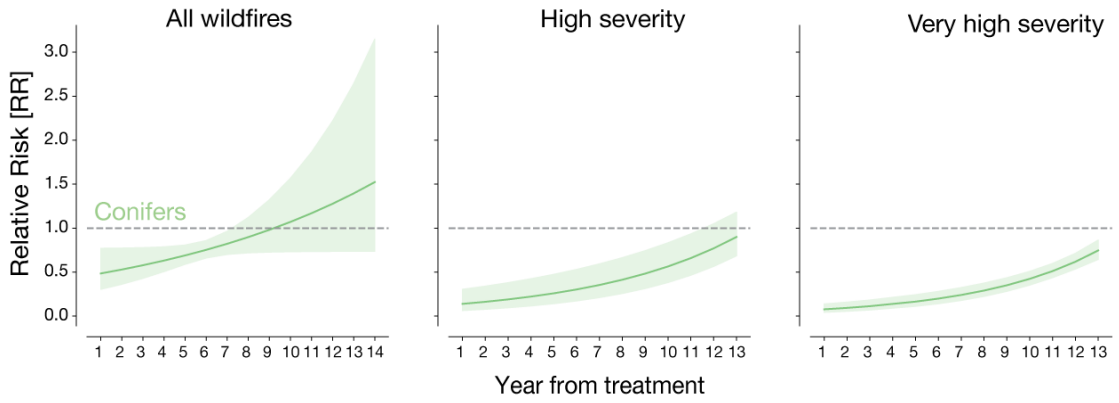

Figure 2: Low severity burning reduces future wildfire risk, with largest declines in extreme fire risk. Estimated impact of low-severity fire exposure in Conifers on subsequent wildfire activity for fires of all severity, high severity, and very high severity. Impact is expressed as relative risk, or the ratio of the outcome in treated pixels to control pixels. Low-severity treatment immediately halves [51.2%, 95% CI: 23.5-70.7] the risk of any wildfire occurring in subsequent years, with this protective effect disappearing after ∼8 years. Protective effects for high and very high severity fires are both large and more persistent, with an immediate 86.2% reduction [95% CI: 70.8 - 93.5%] in severe fire risk that persists for more than a decade.

2 Results

In conifer forests, we find that low-severity treatments reduce risk of any severity wildfire by 52.7% [CI 95%: 23.5 - 70.1%] in the first year after treatment, as compared to matched synthetic controls. This protective effect decays over time but remains statistically significant after seven years for any level of wildfire severity. The protective effects of initial low-severity fire are even stronger for subsequent severe and very severe fire, with immediate reductions in risk of severe (86.2% [CI 95%: 70.8 - 93.5 %]) and very severe (92.4 % [CI 95%: 86.9 - 95.6 %]) wildfires that remain large and statistically significant for at least a decade (Fig 2). This sustained reduction in extreme wildfire risk following low severity fire is consistent with the removal of ground and ladder fuels, the presence of which is known to increase the risk of extreme crown fires [34, 45].

We find mixed evidence for protective effects of low severity fire in other dominant land types in CA. Compared to conifers, where responses to low-severity fire have been explained by a reduction of ladder fuels and fuel density, shrubland vegetation is expected to respond differently to low-severity wildfire. This is both because shrubland has a higher propensity to burn at high-severity [15], and also because rapid fire-fueled re-sprouting that promotes more shrubland growth and the vegetation species displacement after wildfire [26, 15]. Consistent with this expectation, we find a reduction in wildfire risk of 42.2% [CI 95%: 25.5 - 53.3 %] in the first year after treatment in shrubland, but this effect is short-lived compared to the effect in conifers, decaying to zero after four years (Fig S3); we find no statistically significant effect of low-severity fire on future risk of higher-severity fires, although estimates are noisy. We also could not detect a protective effect of low-severity fires in conifer-hardwood or hardwood land types, perhaps in part because of the low presence of low-severity treatments in these areas (Fig S3 and Fig S4).

Estimating spillover benefits of low-severity fire to surrounding unburned areas, we find initially unburned pixels within 2-km of pixels that burned at low severity experience a subsequent reduction in wildfire risk of 43.4% [95% CI: 23.4% - 58.2%] in the first year after exposure to nearby wildfire. As with the effect of

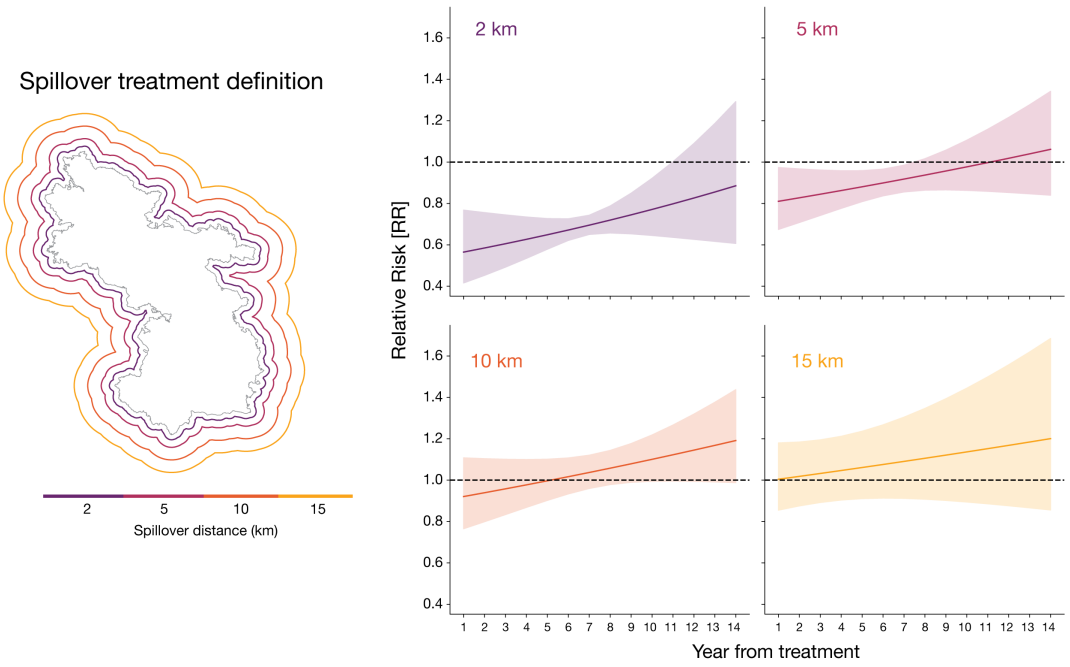

Figure 3: Low-severity wildfire reduces subsequent fire risk in surrounding unburned areas. We re-define "treatment" as unburned pixels proximate to pixels that burned at low severity, and again use synthetic control to track the evolution of future fire risk on comparable controls that were far from burning. For areas immediately adjacent to a wildfire boundary (2 km), fire risk falls immediately by 43% [CI: 58.2 - 23.4 %], with benefits lasting at least twelve years. Impacts decrease at distances further from burned pixels, with non-statistically-significant effects after 5 km. We find similar spillover effects for unburned pixels near pixels that burned at high severity (Fig S7).

direct exposure to wildfire, this "spillover" effect decays within about a decade of exposure (Fig 3). Similar but somewhat more muted effects are present up to 5 km from initially burned pixels, with a immediate risk reduction after the first year of treatment of 24.5% [CI 95%: 10.4% - 36.8%] and a decay to zero after 7-8 years. Past 5 km, we find no statistically significant reductions in subsequent fire risk, consistent with existing literature that suggests such limiting effects are only relevant to locations proximate to previous fires [13, 46]. Results are robust to limiting the sample of fires to the smallest fires in our dataset ($< 4,000$ acres), which perhaps better approximate likely prescribed fire sizes (Fig S12). We find similar spillover effects on reducing the risk of future high-severity and very-high severity fires (Fig S7). We cannot differentiate any of these effects by vegetation type, as pixels beyond the fire boundary can be made up of a variety of vegetation types. When estimating spillovers using absolute changes in ΔNBR instead of relative risk, we find that per-pixel benefits in spillover pixels are roughly one-fourth of the benefits in the treated pixel (Fig S11).

One potential concern is that fire suppression could respond to low severity fire in a way that affects subsequent fire severity, for instance if suppression effort differentially targets previously unburned areas more likely to burn at high severity (biasing treatment effect estimates towards zero), or if suppression activities such as cutting fire lines also directly reduce future fire probability around initially treated pixels (biasing estimates away from zero). However, using fire-level data on suppression costs from [5], we find no relationship between average fire severity and suppression cost per acre (Fig S16A). Similarly, when we restrict our sample to wilderness areas where suppression efforts are typically lower, estimates suggest that low severity fire reduces future fire risk in a way similar to our full sample (Fig S16 C-D). We cautiously conclude that suppression efforts are not likely biasing our estimates.

Estimating the benefits of large-scale fire treatments on fire acreage and air quality A primary goal of our analysis is to understand how large-scale, purposeful application of low-severity fire in CA would alter future wildfire risk and resulting air quality from emitted smoke. This requires an ability to estimate how such treatments would alter subsequent fire activity and severity, which we developed above, with a method for translating changes in fire activity of different severity into changes in population smoke exposure. To accomplish this latter task, we build on earlier work that used satellites and machine learning to measure population smoke exposure from wildfires across the US [12], and related work that uses HYSPLIT (a particle tracer model) [43] to link this smoke back to source fires [53]. We then build a regression model that maps variation in fire-attributed smoke – measured as time- and space-integrated surface PM attributed to a specific source fire (Methods) – to the severity of that fire, accounting for differences in area burned and wildfire duration. As expected, we find that more severe fires generate more smoke, controlling for fire size, with effects increasing roughly linearly with each additional pixel that burns at higher fire severity (Fig S9).

We combine this fire severity-smoke relationship with our estimates of the direct and indirect (spillover) impacts of low-severity fire on subsequent fire risk to calculate the net smoke impacts of a policy that would apply up to 1 million acres per year of low-severity fire to CA conifer forests, analogous to the recently proposed CA state policy goal [11]. Our approach assumes that low-severity wildfire is a good proxy for the prescribed fire treatments that would occur under such a policy. In each year starting in 2010, we randomly allocate low-severity treatments in 1 km^2 ($\approx$ 250 acres) patches across existing conifer forests in CA, assuming the same patch is never treated twice and never treated after a wildfire (Methods SI). Random allocation roughly reflects observed targeting accuracy of the limited number of treatments in the CalFIRE prescribed fires dataset (Figure S20).

We then compute changes in subsequent burn severity using the same causal relationships above (Figures 2, 3, S11), where the benefits of a given treatment only arise if that pixel happened to burn in a subsequent wildfire observed in MTBS; if a treated pixel does not subsequently burn, then the policymaker incurs the smoke cost of the initial treatment without subsequent benefit (Methods SI). Finally, we track pixel-specific burn severity and resulting smoke from this prescribed fire policy, relative to a no-policy counterfactual where each pixel burned at its observed year and severity in the measured ΔNBR data. For each year after policy initiation, we calculate the ratio of discounted cumulative benefits (in terms of reduced smoke) to discounted cumulative costs (the emitted smoke from the prescribed burns in each year), where these costs are assumed to represent health costs from smoke and to scale linearly with smoke exposure, following evidence from a recent meta-analysis [19] (see Discussion). We propagate uncertainty across all steps. We do not account for the financial costs of implementing the fuels treatments themselves.

We simulate the policy both with and without treatment spillovers to nearby unburned areas. In the no-spillover policy, costs and benefits both scale linearly with the amount of area burned - i.e. each treated pixel generates the same amount of initial smoke and same reduction in future smoke, in expectation. The cost/benefit ratio of the policy thus does not depend on the number of treated acres, but the overall benefit in terms of total smoke reduction scales linearly with the number of treated acres. The same pattern roughly holds in the policy with spillovers, except very large treatment policies can actually have slightly diminishing returns, as we effectively run out of acres to treat in CA after a decade of treatments; any treated acre thus incurs the same costs but generates large but diminishing benefits because nearby pixels have already been treated (Fig S13) and cannot benefit twice in our simulation.

We find that even under a conservative assumption of no treatment spillovers to nearby untreated pixels, the expected discounted benefits of treating an acre of conifers with low severity fire, in terms of smoke

reduction, exceed the initial smoke cost after roughly 6-8 years, depending on the discount rate (Fig 4 and S15, left column). At lower discount rates (2%), smoke benefits exceed costs by a factor of four a decade after treatment and are statistically significant. At very high discount rates, net benefits are positive but more uncertain a decade after treatment. Accounting for treatment spillovers of low severity fire to nearby untreated pixels (within 2 km), which our data suggests is warranted, dramatically increases the net smoke benefits of a treatment. Under all discount rates, net impacts are positive within 4 years, statistically significant within 8 years, and net benefit ratios are greater than 10 after a decade (Fig 4, right column).

We then estimate how our simulated prescribed burn policy of treating up to a million acres a year would affect total wildfire acres, the proportion of acres burned at different severity, and the overall contribution of fire to surface smoke PM concentrations. Figure 5A shows predicted total acres (wildfire and prescribed fire) burned per year under a 1 million acres/year (~4,000 km^2/yr) prescribed burn policy, versus what was observed historically. We estimate that 1 million acres/year of prescribed fire treatments in CA would roughly double total wildfire acreage in years with more limited wildfire activity (e.g. 2011-2016), but would reduce total acreage burned in historically active fire years by about 25% (e.g. 2020). Such a treatment policy would also substantially increase the proportion of area burned to low-severity fire in all years, and reduce the proportion burned at high or very high severity fire (Fig 5B).

While our approach does not allow us to precisely quantify the population exposed to smoke under observed and policy counterfactuals, it does allow us to calculate the total change in surface smoke PM attributable to wildfires in CA resulting from an expanded prescribed burn policy in CA. Assuming no treatment spillovers, we estimate that a policy of 1 million acres/year of prescribed burning in CA since 2010 would initially more than double total smoke exposure in the early years of the treatment program, given very low wildfire activity in those years (Fig 5C). We estimate that it would then lead to cumulative reductions in exposure after roughly 8 years, which grow to a 9% [CI 95%: 7.8 - 10.1%] overall reduction in cumulative exposure by 2021. We estimate that this is equivalent to a population-weighted reduction in average annual smoke $PM_{2.5}$ of about $0.3\mu g/m^3$ in 2020 (Fig S18). Cumulative benefits exceed costs slightly later in this exercise as compared to per-acre estimates in Fig 4, as here costs are being incurred repeatedly in each year of the policy as additional acres are treated.

Accounting for treatment spillovers allows for even larger benefits with substantially fewer acres treated. For instance, accounting for spillover benefits out to 2 km from treatments, as our data suggest is warranted, we estimate that a policy of treating only 500 thousand acres/year (~2,000 km^2/yr) would increase initial smoke exposures by 50% in early low-smoke years, but lead to reductions in cumulative smoke exposure as early as year 4, and a 10% reduction after a decade. Larger annual treatments lead to larger cumulative reductions, but with diminishing returns once spillovers are accounted for: at high treatment levels, most acres in CA forests will have received either direct or spillover treatments after a decade, rendering each additional treated acre less beneficial (see Methods).

3 Discussion

Our findings add to a growing literature suggesting the substantial benefits of low-severity and low-intensity fire [55, 34, 45, 27] for reduced future fire risk. Using data on nearly every burned acre in CA over the last two decades, we extend this work to consider the benefits of low severity wildfire across multiple vegetation types, for nearby untreated areas, and for air quality, focusing on measures of fire severity (rather than fire intensity, as in past work [55]) that better map to emissions. We find that not only does direct exposure

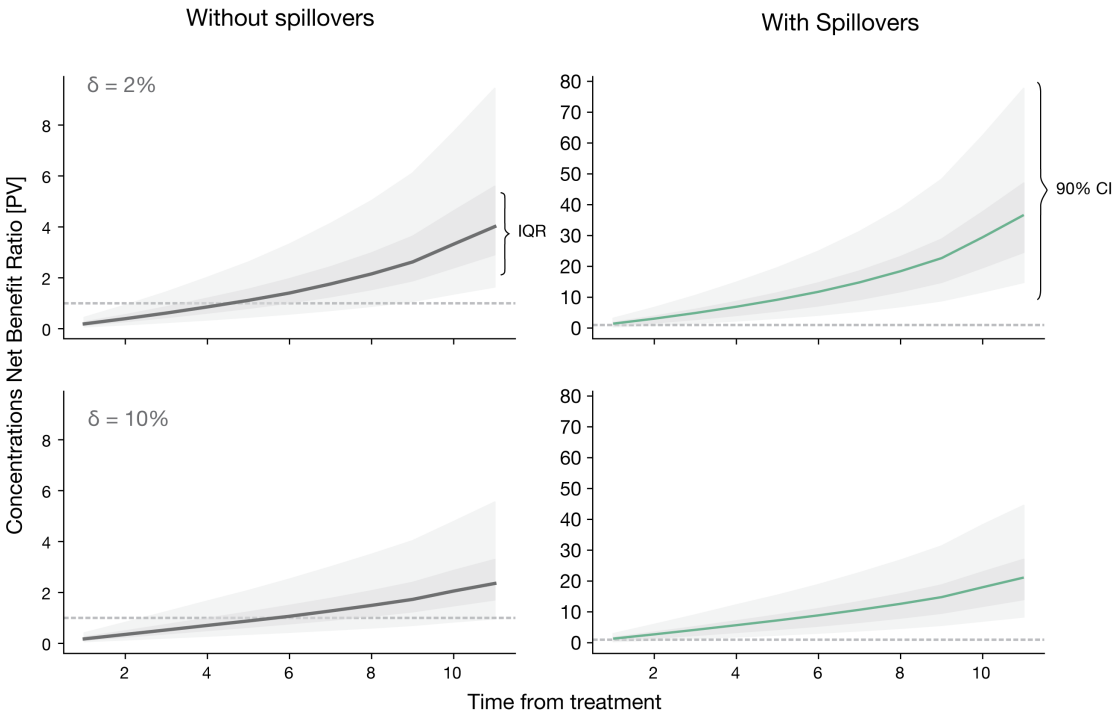

Figure 4: Cumulative ratio of expected costs and benefits, in terms of smoke concentrations, from an acre of prescribed burning. Initial prescribed fire treatment incurs costs, in terms of increasing surface smoke $PM_{2.5}$ concentrations, but results in expected future reductions in smoke concentrations. Estimates show the ratio of cumulative future smoke reductions to initial smoke costs, for a decade after initial treatment. Left column: estimates without accounting for spillover benefits to nearby unburned pixels. Right column: accounting for spillovers within 2 kilometers of a burned pixel. Note different y-axes. Top row: benefits under a 2% annual discount rate; bottom row: benefits under 10% discount rate. The net benefit ratio is positive, large and significant after ten years in all settings, and with positive cumulative benefits after 4-5 years assuming no spillovers, and after 2 years when spillovers are accounted for.

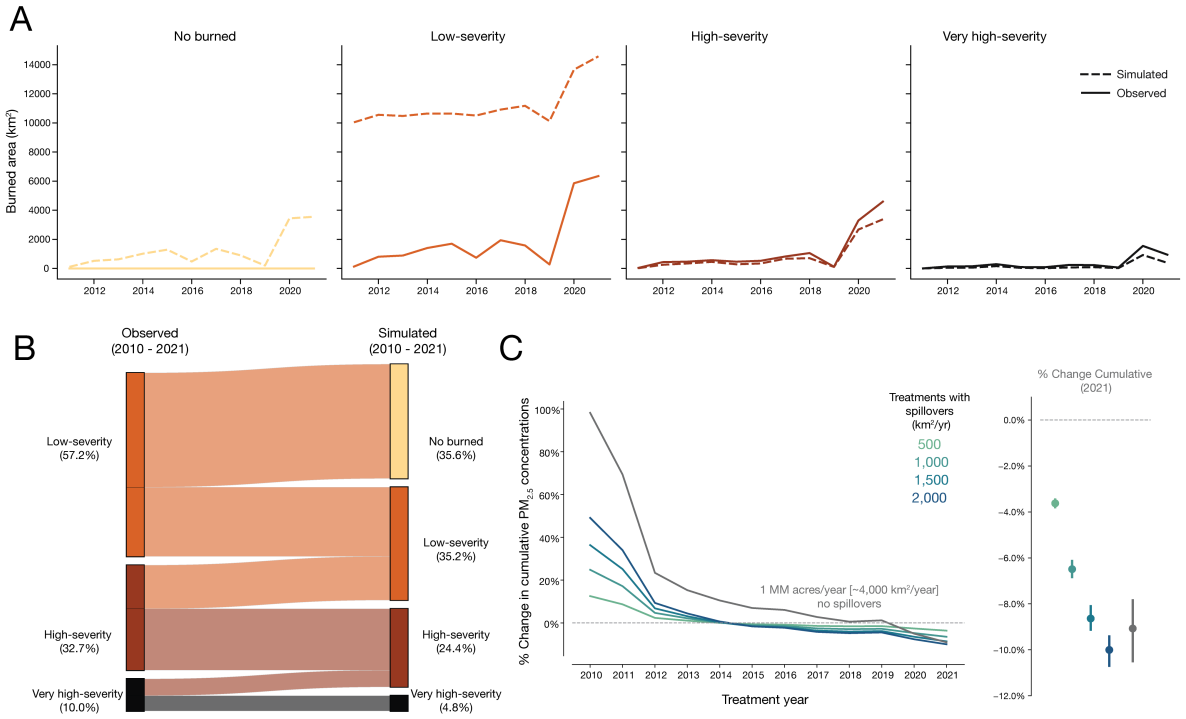

Figure 5: Large-scale prescribed burning reduces future burned area and wildfire smoke $PM_{2.5}$. a. Simulated impacts on total burned area of a policy that treats 1 million conifer acres with prescribed fire each year from 2010 to 2020, assuming no pixels are treated twice and no spillover benefits to nearby untreated pixels. Total burned area at low severity increases in all years, but declines by up to 25% at higher severities in recent extreme wildfire years. **b.** For areas that burned in wildfires, estimated change in the share of area burned to low, high, and very high severity wildfire, under the 1 million acres/yr (~4,000 km^2/yr) treatment policy; estimates do not include additional acres treated by low-severity fire. Large-scale use of low-severity treatments increases the proportion of acres that are identified as non-burning ($\Delta NBR < 0$) and reduces proportions of acreage burning at high and very high severity. **c.** Estimated percent change in cumulative smoke $PM_{2.5}$ under different levels of low-severity treatment, as a proportion of the total observed smoke $PM_{2.5}$. Treatment scenarios include the 1 million acres/year with no spillover benefits (gray), as well as alternative spillovers scenarios that treat from 500 to 2,000 km^2 (125-500 thousand acres) annually and include spillover benefits out to 2 km from each treated pixel (blue colors). Dot-and-whisker plot at right shows point estimate and 95% CI for cumulative benefits by 2021, for each scenario.

to low-severity fires significantly reduce risk of subsequent severe fires in conifer systems, but also that this exposure has large spillovers benefits, in terms of reduced probability of future severe fire for nearby (2-5 km) untreated pixels. While our work is the first to identify these spillovers statistically at large spatial scale and across many fires, it is consistent with other case study evidence that suggests fires limit subsequent fire in nearby areas [35, 46, 37]. We cannot identify this risk reduction in other dominant vegetation types, such as Conifer-Hardwood and Hardwood, as we do not have a large enough sample of low-severity fires to explore this relationship in these settings. Similarly, we find that the response of shrubland and other chaparral systems to low-severity treatments is uncertain, aligning with similar observations that show these systems have much longer natural fire return intervals and often higher severity fires when they occur [15]. Together, these results suggest that simply keeping fire from entering chaparral systems could be more effective than the purposeful use of low-severity fire in limiting impacts of fire on surrounding communities.

Our results on the reduction in risk of high severity fire following low severity fire are plausibly the result of low severity fire itself and not well explained by simple mean reversion. First, our synthetic control approach is able to closely match treated pixels to untreated controls that should have the same probability of fire in each year. Second, spillover effects observed in nearby untreated areas are consistent with localized reductions in available fuel loads extending beyond burn perimeters. Third, stronger and more persistent treatment effects in Conifers relative to Shrublands align with the ecological mechanism of slower fuel recovery [26, 15], again suggesting that fuel depletion, rather than regression to the mean, explains our result. Finally, our results align with long-term experimental data that finds a consistent fuel reduction up to seven years after low-severity treatments [44], and that finds shadow effects from treatments in conifers areas [30].

Since low-severity fires are a reasonable proxy for prescribed fire burning severity in conifer forests (Fig S10), we use our estimates from low-severity wildfire to simulate a policy where California applies prescribed burning at large scale in the state's conifer forests (up to 1 million acres/year). We found for a policymaker embarking on this policy, cumulative benefits in terms of smoke reduction would exceed the costs of the added smoke from the initial acreage burned prescribed burning in as early as two years, with benefits exceeding costs by at least three-fold a decade after project initiation. These results are comparable to recent monetized damages estimate that suggests a similar three-fold increase in treatment benefits over burning costs after a single year of treatment [8], although these results do not include air-quality considerations or the potential negative health impacts of prescribed fires [2].

Our approach to linking changes in fire activity to resulting smoke relies on a statistical mapping of observed fires to satellite-estimated smoke. An alternate approach would be to couple emissions inventory data on low-severity or prescribed fire with chemical transport models to estimate resulting smoke changes. However, existing work shows that inventory and transport-model-based estimates of wildfire smoke are largely unable to reliably reproduce observed surface wildfire smoke concentrations in the US, raising questions about their applicability in this context [29, 39]. While our statistical approach allows us to quantify and propagate uncertainty in how changes in fire activity affect total smoke concentrations, further refinements of this approach could further reduce uncertainty and improve confidence in our estimated smoke changes.

Our results depend on a number of key assumptions. First, our simulation on potential smoke reductions from prescribed burning assumes that treatments are applied exclusively to only conifers, where we have identified large causal effects. Second, we assume that the policymaker does not target treatments but instead applies them randomly to conifer forests across the state without treating them again. To the extent that better targeting is possible – e.g to very high risk fire areas – this implies that our estimates are likely lower bounds on benefits [17, 16]. We estimate that targeting success of observed prescribed burn

treatments in CA, in terms of treating areas that later overlap with wildfire, (Methods SI) is on average close to random allocation (Fig S20), suggesting that improvements over the current targeting will be needed to improve policy benefits beyond what we estimate here. Third, we assume pixels are never treated twice, which implies that the beneficial treatment effects will wane over time and disappear after roughly a decade. A policy of re-treating pixels could sustain benefits but would also incur some costs, although smoke emissions could be meaningfully lower in subsequent treatments. Fourth, our estimates of benefits and costs of smoke assume that a unit of wildfire smoke and a unit of smoke from prescribed fire have equivalent costs – specifically, that a $1\mu g/m^3$ increase in either has the same health impact. We know of no reliable population health evidence on this equivalence. Existing health impact studies assume equivalent dose-specific impacts [2, 22] and we make the same assumption. Fifth, our estimates of the spillover benefit of low-severity fire to nearby unburned pixels derive from a purposefully-limited subsample of remote fires where other human influences (e.g. roads) are largely removed. As a result, our estimated spillover benefits could be an upper bound on true benefits in settings where these human influences limit fire spread. Sixth, prescribed fires are often combined with other non-emitting fuel treatments, such as mechanical thinning. In combination, both treatments tend to be more effective that burning [45, 36] or thinning alone [27]. Thus our estimates could be an underestimation of the benefits of prescribed fire if an enacted policy combines both treatment types. Finally, our results assume that prescribed fires are always contained. While the probability of escaped treatments is low (close to 2% [18]), high-profile recent escapes such as the 2022 Calf Canyon-Hermits Peak Fire in New Mexico which burned more than 260,000 acres, along with more limited weather windows for successful treatments due to climate change [47], suggests that escapes will be an ongoing concern, particular as the scale of treatments is ramped up.

Our results could be combined with recent evidence on the mortality [41] and morbidity [20, 21, 19] impacts of wildfire smoke exposure to estimate the specific health damages or benefits from expanded use of prescribed fire. For health outcomes that are roughly linear in smoke exposure (e.g. asthma cases [21, 19]), health benefits will scale directly with overall changes in smoke. If smoke-health dose-response functions are nonlinear, however, as existing work sometimes indicates, reliably estimating health damages will require more precise (e.g. zip-code or county-level) estimates of location-specific smoke impacts from prescribed burning treatments than our current approach can provide. Transport-model-based approaches are an alternative tool to help inform local-level smoke impacts, but such approaches have also not yet proven a reliable tool for estimating surface PM smoke concentrations from existing wildfire emissions inventories [39]. Innovation in this area will be critical for fully characterizing the health benefits of expanded prescribed fire treatments. Nevertheless, despite uncertainty in the magnitude of monetized benefits, our results strongly suggest that a given quantity of prescribed burning yields a large net reduction in overall smoke exposure, and that a sustained policy of large-scale prescribed burning is likely to meaningfully reduce state-wide smoke concentrations, especially in high-wildfire years.

References

[1] John T. Abatzoglou and A. Park Williams. "Impact of anthropogenic climate change on wildfire across western US forests". In: *Proceedings of the National Academy of Sciences* 113.42 (Oct. 2016), pp. 11770–11775. DOI: 10.1073/pnas.1607171113.

[2] Sadia Afrin and Fernando Garcia-Menendez. "Potential impacts of prescribed fire smoke on public health and socially vulnerable populations in a Southeastern U.S. state". In: *Science of The Total Environment* 794 (Nov. 2021), p. 148712. ISSN: 0048-9697. DOI: 10.1016/j.scitotenv.2021.148712.

[3] James K. Agee and Carl N. Skinner. "Basic principles of forest fuel reduction treatments". In: *Forest Ecology and Management*. Relative Risk Assessments for Decision –Making Related To Uncharacteristic Wildfire 211.1 (June 2005), pp. 83–96. ISSN: 0378-1127. DOI: 10.1016/j.foreco.2005.01.034.

[4] Rosana Aguilera et al. "Wildfire smoke impacts respiratory health more than fine particles from other sources: observational evidence from Southern California". en. In: *Nature Communications* 12.1 (Mar. 2021), p. 1493. ISSN: 2041-1723. DOI: 10.1038/s41467-021-21708-0.

[5] Patrick Baylis and Judson Boomhower. "The Economic Incidence of Wildfire Suppression in the United States". en. In: *American Economic Journal: Applied Economics* 15.1 (Jan. 2023), pp. 442–473. ISSN: 1945-7782. DOI: 10.1257/app.20200662.

[6] Matthias M. Boer et al. "Long-term impacts of prescribed burning on regional extent and incidence of wildfires—Evidence from 50 years of active fire management in SW Australian forests". In: *Forest Ecology and Management* 259.1 (Dec. 2009), pp. 132–142. ISSN: 0378-1127. DOI: 10.1016/j.foreco.2009.10.005.

[7] Mark Borgschulte, David Molitor, and Eric Zou. "Air Pollution and the Labor Market: Evidence from Wildfire Smoke". en. In: (Apr. 2022), w29952. DOI: 10.3386/w29952.

[8] Patrick Brown. *Cost-Effectiveness of Large-scale Fuel Reduction for Wildfire Mitigation in California*. Breakthrough Institute Working Paper, 2025.

[9] Marshall Burke et al. "The changing risk and burden of wildfire in the United States". In: *Proceedings of the National Academy of Sciences* 118.2 (Jan. 2021), e2011048118. DOI: 10.1073/pnas.2011048118.

[10] Marshall Burke et al. "The contribution of wildfire to PM2.5 trends in the USA". en. In: *Nature* 622.7984 (Oct. 2023), pp. 761–766. ISSN: 1476-4687. DOI: 10.1038/s41586-023-06522-6.

[11] California Wildfire & Forest Resilience Task Force. "California's Strategic Plan for Expanding the Use of Beneficial Fire". en. In: (Mar. 2022).

[12] Marissa L. Childs et al. "Daily Local-Level Estimates of Ambient Wildfire Smoke PM2.5 for the Contiguous US". In: *Environmental Science & Technology* 56.19 (Oct. 2022), pp. 13607–13621. ISSN: 0013-936X. DOI: 10.1021/acs.est.2c02934.

[13] Brandon M. Collins et al. "Interactions Among Wildland Fires in a Long-Established Sierra Nevada Natural Fire Area". en. In: *Ecosystems* 12.1 (Feb. 2009), pp. 114–128. ISSN: 1435-0629. DOI: 10.1007/s10021-008-9211-7.

[14] L. Collins et al. "Fuel reduction burning reduces wildfire severity during extreme fire events in south-eastern Australia". In: *Journal of Environmental Management* 343 (Oct. 2023), p. 118171. ISSN: 0301-4797. DOI: 10.1016/j.jenvman.2023.118171.

[15] Michelle Coppoletta, Kyle E. Merriam, and Brandon M. Collins. "Post-fire vegetation and fuel development influences fire severity patterns in reburns". en. In: *Ecological Applications* 26.3 (2016), pp. 686–699. ISSN: 1939-5582. DOI: 10.1890/15-0225.

[16] Kristofer L. Daum et al. "Do Vegetation Fuel Reduction Treatments Alter Forest Fire Severity and Carbon Stability in California Forests?" en. In: *Earth's Future* 12.3 (2024), e2023EF003763. ISSN: 2328-4277. DOI: 10.1029/2023EF003763.

[17] Alison L. Deak et al. "Prescribed fire placement matters more than increasing frequency and extent in a simulated Pacific Northwest landscape". en. In: *Ecosphere* 15.4 (2024), e4827. ISSN: 2150-8925. DOI: 10.1002/ecs2.4827.

[18] Deirdre Dether and Anne Black. "Learning from Escaped Prescribed Fires – Lessons for High Reliability". In: *Fire Management Today* 66.4 (2006), pp. 50–56.

[19] Carlos F. Gould et al. "Health Effects of Wildfire Smoke Exposure". en. In: *Annual Review of Medicine* 75.Volume 75, 2024 (Jan. 2024), pp. 277–292. ISSN: 0066-4219, 1545-326X. DOI: 10.1146/annurev-med-052422-020909.

[20] Sam Heft-Neal et al. "Associations between wildfire smoke exposure during pregnancy and risk of preterm birth in California". In: *Environmental Research* 203 (Jan. 2022), p. 111872. ISSN: 0013-9351. DOI: 10.1016/j.envres.2021.111872.

[21] Sam Heft-Neal et al. "Emergency department visits respond nonlinearly to wildfire smoke". In: *Proceedings of the National Academy of Sciences* 120.39 (Sept. 2023), e2302409120. DOI: 10.1073/pnas.2302409120.

[22] Ran Huang et al. "The Impacts of Prescribed Fire on PM2.5 Air Quality and Human Health: Application to Asthma-Related Emergency Room Visits in Georgia, USA". In: *International Journal of Environmental Research and Public Health* 16.13 (July 2019), p. 2312. ISSN: 1661-7827. DOI: 10.3390/ijerph16132312.

[23] Timothy Ingalsbee. "Whither the paradigm shift? Large wildland fires and the wildfire paradox offer opportunities for a new paradigm of ecological fire management". en. In: *International Journal of Wildland Fire* 26.7 (July 2017), pp. 557–561. ISSN: 1448-5516. DOI: 10.1071/WF17062.

[24] Daniel A. Jaffe et al. "Wildfire and prescribed burning impacts on air quality in the United States". In: *Journal of the Air & Waste Management Association* 70.6 (June 2020), pp. 583–615. ISSN: 1096-2247. DOI: 10.1080/10962247.2020.1749731.

[25] Michael Jerrett, Amir S. Jina, and Miriam E. Marlier. "Up in smoke: California's greenhouse gas reductions could be wiped out by 2020 wildfires". In: *Environmental Pollution* 310 (Oct. 2022), p. 119888. ISSN: 0269-7491. DOI: 10.1016/j.envpol.2022.119888.

[26] J. E. Keeley. "Fire". In: *Encyclopedia of Ecology*. Ed. by Sven Erik Jørgensen and Brian D. Fath. Oxford: Academic Press, Jan. 2008, pp. 1557–1564. ISBN: 978-0-08-045405-4. DOI: 10.1016/B978-008045405-4.00496-1.

[27] Makoto Kelp et al. "Effect of Recent Prescribed Burning and Land Management on Wildfire Burn Severity and Smoke Emissions in the Western United States". en. In: *AGU Advances* 6.3 (2025), e2025AV001682. ISSN: 2576-604X. DOI: 10.1029/2025AV001682.

[28] Makoto M. Kelp et al. "Data-Driven Placement of PM2.5 Air Quality Sensors in the United States: An Approach to Target Urban Environmental Injustice". en. In: *GeoHealth* 7.9 (2023), e2023GH000834. ISSN: 2471-1403. DOI: 10.1029/2023GH000834.

[29] Shannon N. Koplitz et al. "Influence of uncertainties in burned area estimates on modeled wildland fire PM2.5 and ozone pollution in the contiguous U.S." In: *Atmospheric Environment* 191 (Oct. 2018), pp. 328–339. ISSN: 1352-2310. DOI: 10.1016/j.atmosenv.2018.08.020.

[30] Kathryn E. Low et al. "Shaded fuel breaks create wildfire-resilient forest stands: lessons from a long-term study in the Sierra Nevada". In: *Fire Ecology* 19.1 (May 2023), p. 29. ISSN: 1933-9747. DOI: 10.1186/s42408-023-00187-2.

[31] Jamie M. Lydersen et al. "Evidence of fuels management and fire weather influencing fire severity in an extreme fire event". en. In: *Ecological Applications* 27.7 (2017), pp. 2013–2030. ISSN: 1939-5582. DOI: 10.1002/eap.1586.

[32] Kamal J. Maji et al. "Estimated Impacts of Prescribed Fires on Air Quality and Premature Deaths in Georgia and Surrounding Areas in the US, 2015–2020". In: *Environmental Science & Technology* 58.28 (July 2024), pp. 12343–12355. ISSN: 0013-936X. DOI: 10.1021/acs.est.4c00890.

[33] S. A. Parks and J. T. Abatzoglou. "Warmer and Drier Fire Seasons Contribute to Increases in Area Burned at High Severity in Western US Forests From 1985 to 2017". en. In: *Geophysical Research Letters* 47.22 (Nov. 2020), e2020GL089858. ISSN: 0094-8276, 1944-8007. DOI: 10.1029/2020GL089858.

[34] Sean A. Parks et al. "Previous Fires Moderate Burn Severity of Subsequent Wildland Fires in Two Large Western US Wilderness Areas". en. In: *Ecosystems* 17.1 (Jan. 2014), pp. 29–42. ISSN: 1432-9840, 1435-0629. DOI: 10.1007/s10021-013-9704-x.

[35] Sean A. Parks et al. "Wildland fire limits subsequent fire occurrence". en. In: *International Journal of Wildland Fire* 25.2 (Nov. 2015), pp. 182–190. ISSN: 1448-5516. DOI: 10.1071/WF15107.

[36] Susan J. Prichard and Maureen C. Kennedy. "Fuel treatment effects on tree mortality following wildfire in dry mixed conifer forests, Washington State, USA". In: *International Journal of Wildland Fire* 21.8 (Aug. 2012), pp. 1004–1013. ISSN: 1049-8001. DOI: 10.1071/WF11121.

[37] Susan J. Prichard, Camille S. Stevens-Rumann, and Paul F. Hessburg. "Tamm Review: Shifting global fire regimes: Lessons from reburns and research needs". In: *Forest Ecology and Management* 396 (July 2017), pp. 217–233. ISSN: 0378-1127. DOI: 10.1016/j.foreco.2017.03.035.

[38] Susan J. Prichard et al. "Adapting western North American forests to climate change and wildfires: 10 common questions". en. In: *Ecological Applications* 31.8 (2021), e02433. ISSN: 1939-5582. DOI: 10.1002/eap.2433.

[39] Minghao Qiu et al. "Evaluating Chemical Transport and Machine Learning Models for Wildfire Smoke PM2.5: Implications for Assessment of Health Impacts". In: *Environmental Science & Technology* 58.52 (Dec. 2024), pp. 22880–22893. ISSN: 0013-936X. DOI: 10.1021/acs.est.4c05922.

[40] Minghao Qiu et al. *Mortality Burden From Wildfire Smoke Under Climate Change*. Working Paper. Apr. 2024. DOI: 10.3386/w32307.

[41] Minghao Qiu et al. "Wildfire smoke exposure and mortality burden in the USA under climate change". en. In: *Nature* (Sept. 2025), pp. 1–9. ISSN: 1476-4687. DOI: 10.1038/s41586-025-09611-w.

[42] Martin W. Ritchie, Carl N. Skinner, and Todd A. Hamilton. "Probability of tree survival after wildfire in an interior pine forest of northern California: Effects of thinning and prescribed fire". In: *Forest Ecology and Management* 247.1 (Aug. 2007), pp. 200–208. ISSN: 0378-1127. DOI: 10.1016/j.foreco.2007.04.044.

[43] A. F. Stein et al. "NOAA's HYSPLIT Atmospheric Transport and Dispersion Modeling System". en. In: *Bulletin of the American Meteorological Society* 96.12 (Dec. 2015), pp. 2059–2077. ISSN: 0003-0007, 1520-0477. DOI: 10.1175/BAMS-D-14-00110.1.

[44] Scott L. Stephens, Brandon M. Collins, and Gary Roller. "Fuel treatment longevity in a Sierra Nevada mixed conifer forest". In: *Forest Ecology and Management* 285 (Dec. 2012), pp. 204–212. ISSN: 0378-1127. DOI: 10.1016/j.foreco.2012.08.030.

[45] Scott L. Stephens et al. "The Effects of Forest Fuel-Reduction Treatments in the United States". In: *BioScience* 62.6 (June 2012), pp. 549–560. ISSN: 0006-3568. DOI: 10.1525/bio.2012.62.6.6.

[46] Camille S. Stevens-Rumann et al. "Prior wildfires influence burn severity of subsequent large fires". In: *Canadian Journal of Forest Research* 46.11 (Nov. 2016), pp. 1375–1385. ISSN: 0045-5067. DOI: 10.1139/cjfr-2016-0185.

[47] Daniel L. Swain et al. "Climate change is narrowing and shifting prescribed fire windows in western United States". en. In: *Communications Earth & Environment* 4.1 (Oct. 2023), pp. 1–14. ISSN: 2662-4435. DOI: 10.1038/s43247-023-00993-1.

[48] Alan H Taylor, Lucas B Harris, and Carl N Skinner. "Severity patterns of the 2021 Dixie Fire exemplify the need to increase low-severity fire treatments in California's forests". en. In: *Environmental Research Letters* 17.7 (June 2022), p. 071002. ISSN: 1748-9326. DOI: 10.1088/1748-9326/ac7735.

[49] Alan H. Taylor, Lucas B. Harris, and Stacy A. Drury. "Drivers of fire severity shift as landscapes transition to an active fire regime, Klamath Mountains, USA". en. In: *Ecosphere* 12.9 (2021), e03734. ISSN: 2150-8925. DOI: 10.1002/ecs2.3734.

[50] Alan H. Taylor et al. "Socioecological transitions trigger fire regime shifts and modulate fire–climate interactions in the Sierra Nevada, USA, 1600–2015 CE". In: *Proceedings of the National Academy of Sciences* 113.48 (Nov. 2016), pp. 13684–13689. DOI: 10.1073/pnas.1609775113.

[51] Casey C. Teske, Carl A. Seielstad, and Lloyd P. Queen. "Characterizing Fire-on-Fire Interactions in Three Large Wilderness Areas". en. In: *Fire Ecology* 8.2 (Aug. 2012), pp. 82–106. ISSN: 1933-9747. DOI: 10.4996/fireecology.0802082.

[52] Jeff Wen and Marshall Burke. "Lower test scores from wildfire smoke exposure". en. In: *Nature Sustainability* 5.11 (Nov. 2022), pp. 947–955. ISSN: 2398-9629. DOI: 10.1038/s41893-022-00956-y.

[53] Jeff Wen et al. "Quantifying fire-specific smoke exposure and health impacts". In: *Proceedings of the National Academy of Sciences* 120.51 (Dec. 2023), e2309325120. DOI: 10.1073/pnas.2309325120.

[54] G. J. Williamson et al. "A transdisciplinary approach to understanding the health effects of wildfire and prescribed fire smoke regimes". en. In: *Environmental Research Letters* 11.12 (Dec. 2016), p. 125009. ISSN: 1748-9326. DOI: 10.1088/1748-9326/11/12/125009.

[55] Xiao Wu et al. "Low-intensity fires mitigate the risk of high-intensity wildfires in California's forests". In: *Science Advances* 9.45 (Nov. 2023), eadi4123. DOI: 10.1126/sciadv.adi4123.

[56] Qingyuan Zhao. "Covariate balancing propensity score by tailored loss functions". In: *The Annals of Statistics* 47.2 (Apr. 2019), pp. 965–993. ISSN: 0090-5364, 2168-8966. DOI: 10.1214/18-AOS1698.

Methods

Our study has three main empirical components: (1) a high-resolution measurement of fire severity across all wildfires over the years 2008-2021; (2) a causal estimation of the impacts of low-severity fire on subsequent fire probability and severity; (3) a estimation of the air quality costs and benefits of a simulated prescribed burn policy. We describe each of these in turn.

S1 Wildfire severity measurement

Fire severity measurement To capture the impact of wildfires on land and vegetation, we use the differenced Normalized Burned Ratio (ΔNBR) [15], a satellite-derived fire severity index that measures the change in above and below ground biomass for each fire perimeter in the Monitoring Trends in Burning Severity (MTBS) dataset [13] between 2000 and 2021 in California. The ΔNBR index compares the Normalized Burned Ratio (NBR) in two different periods, before and after fire, subtracting the post-period from the pre-period, capturing the changes in vegetation explained by fire exposure; higher values of ΔNBR are associated with increased char, consumed fuels, and exposure of mineral soil, and have been shown to be associated with field assessments of burn severity [15]. Following [16], we calculate the ΔNBR using a spatial offset defined as:

$$\Delta NBR = NBR_i^{(pre)} - NBR_i^{(post)} - \text{offset}_i$$

where we define pre-period and post-period as the fire seasons from the previous and next year from the fire ignition year, respectively.

We calculate ΔNBR using imagery from Landsat. For each period, we collect all the overlapping imagery available from Landsat (Collection 2) and calculate the mean composite for the respective fire seasons; we discard all Landsat-7 ETM+ images to avoid data gaps from the Scan Line Corrector (SLC) failure and calculate the composites with single sensor images only whenever is possible. The spatial offset is defined as the average ΔNBR in a 180-meter ring around the perimeter of the wildfire. This offset captures the differences in vegetation phenology and meteorological conditions between periods, allowing a better comparison of severity between fires.

As suggested by [14] and [17], the ability of ΔNBR to accurately measure fire severity can be affected by the speed with which vegetation re-sprouts after fire; this is particularly relevant for shrubland, where crown fires are frequent. We address this concern by making the post-period measurement as close to the fire event as possible, as depicted in Figure S1. Using this pipeline, we achieved a 94% coverage of the fires included in the MTBS dataset in the 2001 to 2021 time frame. Our causal and benefit simulation results are robust to this choice about observation window.

S2 Causal estimation of the impacts of low-severity fire

To quantify the effect of low-severity wildfire treatments ($100 \leq \Delta NBR < 270$, following [15]) on the future risk of very severe wildfire and severity, we calculate outcomes for two different treatment samples: the average reduction in future severity among pixels directly treated by low-severity fire, and the same reduction

for unburned pixels nearby pixels treated with low-severity fire. To measure both causal estimates, we use pre-treatment covariate data to build synthetic controls for each fire treatment period. In this section we will summarize the process of building a valid treatment counterfactual in our setting.

Synthetic control methods (SC) have become widely adopted in social sciences [1, 2, 7] and epidemiology [9] as a way to address the fundamental problem of causal inference [20], or the inability to observe the outcomes of the treated units having not received the treatment. Since its initial introduction by [3], these methods have inspired new research in causal panel data [5] and become an alternative to panel difference-in-differences estimators that rely on strong assumptions about treatment homogeneity and time-varying confounders [6]. In essence, SC methods work by generating a synthetic control group from a unique convex weighting of possible control units with the goal of constructing a control group that closely resembles the treated units in pre-treatment covariates and/or outcomes. Treatment effects are then estimated by comparing treated units to synthetic controls post-treatment. As described below, to balance treated pixels to comparable non-treated controls, we use both pre-treatment outcomes and covariates: a treated and synthetic control pixel are required to have no burning in the 8 years prior to treatment and similar cumulative fire severity prior to that, and similar values of the fire-predictive covariates described in section S2.5.

S2.1 Set up

Let $i \in N$ be a 1 km^2 pixel from a sample of forested pixels in California between 2000 and 2021 indexed in time by $t \in T$. We define the treatment assignment A_{i,T_0} as the pixel exposure to low-severity fire on the treatment period T_0, which we call the "focal year"; this assignment is binary and absorbing, i.e once treated we always consider a pixel treated. Denote $Y_{i,T_0+t}(a)$ the potential outcome in a future period $T_0 + t$, relative to the focal year where $t \in (1, \ldots, T)$. We are interested in two types of estimates: (i) the total change in outcomes $Y_{i,T_0+t}(a)$ captured by the average treatment effect (ATT) defined in Equation 2, and (ii) the change in relative risk after a low-severity fire exposure for each year of exposure (a) and lag (t), which can be interpreted as the percent change in fire frequency [27]:

$$RR(a,t) = \frac{\mathbb{E}[Y_{i,t-a}(1)|A_{it} = 1]}{\mathbb{E}[Y_{i,t-a}(0)|A_{it} = 0]} \tag{1}$$

$$ATT(a,t) = \mathbb{E}[Y_{i,t-a}(1) - Y_{i,t-a}(0)|A_i = a] \tag{2}$$

For both estimators described above, we are comparing the outcomes of treated pixels in period t and the outcome had the pixels not received the treatment in a. Thus, they capture the effects in t of adopting the treatment in the focal year (a). Because the units in the ATT (2) are less interpretable (they are in units of ΔNBR), we estimate RR using count of wildfire events as the outcome, such that $\widehat{RR}(a,t)$ is the number of treated pixels that had a wildfire (high or very high severity) in year t over the number of synthetic controls that had wildfire (high or very high severity) in that same year. Thus an estimate of $\widehat{RR}(a,t) = 0.5$ suggests that in year t, pixels that were treated in year a were 50% less likely to experience high/very high severity wildfire compared to synthetic control pixels.

S2.2 Estimation: Cohort Synthetic Control

Building on earlier work [27], we use a SC approach to calculate the estimates defined above. To calculate the estimands defined in 1 and 2, we search for a set of control units that balances pixels covariates' and outcomes' historical time series and can serve as a set of control observations for any treatment in a focal

year T_0. This approach resembles the ideal experiment where we assign A_i randomly in our sample and evaluate the effects in the next periods. To find the set of optimal weights to create a control group $(\omega_{i,a} \forall i \in N_c)$ for pixels treated in T_0, we follow [29] and [28] and find a set of balancing weights that reduces the distance between the intervention (N_t) and control groups (N_c) covariates' monthly time series prior to treatment. To do this, we use a set of covariates that combines time-series $(x_{i,t-a})$ and static features (x_i) for each observation unit for at least eight years before the focal period, as defined in 3.

$$\boldsymbol{X} = \{x_{i,t_0-8}, x_{i,t_0-7}, \ldots, x_{i,t_0-2}, x_{i,t_0-1}, x_i\} \tag{3}$$

Assuming a linear outcome model and a logistic propensity score $e(x) = {}^{1}/_{1+e^{-x\theta}}$, we want to find of set of ω_i weights that can approximate the covariate trajectories of both exposed and unexposed units for a particular focal period T_0:

$$\frac{1}{n}\sum_{i=1}^{n}(1 + e^{-X\hat{\theta}})\omega_{i,a}\boldsymbol{X}_i \approx \frac{1}{n}\sum_{i=1}^{n}\boldsymbol{X}_i \tag{4}$$

Notice that 4 is defining the first-order conditions for the following optimization problem:

$$\begin{aligned} \hat{\theta} &= \arg\min_{\theta}\left\{\frac{1}{n}\sum_{i=1}^{n}\ell_\theta(\boldsymbol{X}_i, \omega_{i,a})\right\} \\ \ell_\theta(\boldsymbol{X}_i, \omega_i) &= \omega_{i,a}e^{-\boldsymbol{X}_i\theta} + (1-\omega_{i,a})\boldsymbol{X}_i\theta + \lambda\|\theta\|_2 \end{aligned} \tag{5}$$

We estimate 5 using gradient descent (`AdamW`) with a L_2 regularization. We use a grid search to find the regularization (λ) and learning rate (α) parameters that better minimize our objective loss (ℓ_θ).

Following [27], we estimate balancing weights for each intervention year, or focal year (a), and use these to calculate the effects of the intervention in time a onto the next periods $(a + t)$. We select the best model for each focal year a using the set of parameters with that minimize ℓ_θ for that year. The figure below shows an example of the estimation process starting in 2008 as the focal year, where we estimate a SC group using a set of weights $\omega_{i,2008}$ using all the covariates $X_{i,a<2008}$ before in the pre-treatment period, and evaluate the causal effects after the focal year. We repeat this process for each year from 2008 to 2020, making sure that we always have at least 8 years of covariates.

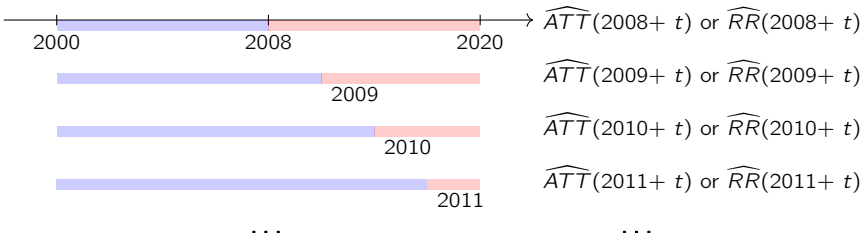

SC cohort design: timeline of estimations using synthetic control. In this example, we estimate different set of control groups for each focal year in our sample starting from 2008. In this example, all pre-treatment years are the pre-focal period, and all the years after 2015 the treatment we call evaluation periods. We estimate a different synthetic control (SC) for each intervention year in the sample $a \in A_i = \{2000, \ldots, 2020\}$, leaving a set of minimum 8 years to do covariate balancing. For each SC, we calculate the lagged effects from the current treatment in 2015 to the future t: $\widehat{ATT}(2015, t)$.

We estimate a set of weights $\omega_{i,a}$ for each focal year a to obtain a set of "as-random" control observations of size N_c^a that is comparable to the pixels exposed to low degree fire in period a, N_t^a to calculate the effects in future periods $(a+t)$ using the sample analog estimators of 1 and 2.

$$\widehat{ATT}(a,t) = \frac{1}{N_t^a}\sum_{i=1}^{N_t} Y_{i,a,t} - \frac{1}{N_c^a}\sum_{i=1}^{N_c} \omega_{i,a} Y_{i,a,t} \tag{6}$$

$$\widehat{RR}(a,t) = \frac{\mathbb{E}[Y_{i,t-a}(1)|\omega_{i,a}=1]}{\mathbb{E}[Y_{i,t-a}(0)|\omega_{i,a}=0]} \tag{7}$$

S2.3 Inference

Having estimated SC weights for all the focal years from 2008 to 2020 (a'), we can use these to calculate treatment effects for all the outcome years in the evaluation period after the focal year ($a' > a$). We show these estimates for the risk ratio estimator for Conifers in Figure S5, where the point size captures the precision of each estimate. Variation in precision is driven by variation over time in the observed frequency of fire types of different severities; in years with low fire activity, such as 2015 and 2016, relative risk estimates are imprecise. To improve the interpretability of these effects, and following [27], we pool the estimates using a log-linear relationship (Eq 8) using all the estimates across focal year (a) and lags after treatment (t) using a weighted quasi-Poisson regression, where we weight each RR estimate by the number of burned pixels at a given severity within the SC group for t period.

$$\log \widehat{RR}(a,t) = \alpha + \beta \cdot t + \varepsilon_i \tag{8}$$

We calculate the standard errors of β using jackknife standard errors where we cluster all observations within a particular lag (t). This leave-one-out sampling process accounts for the variation in fire activity across the focal years and the fact that a pixel observation can be both part of a SC in one lag and a treated pixel for another lag. We follow a similar approach to pool the $\widehat{ATT}$. For these estimates, we assume a linear relationship between the average effects and the lags using a weighted OLS, using the individual variances of each $\widehat{ATT}$ as weights in the regression. Just as with the risk ratio estimation, where the estimator precision can vary across focal years and where we assume a particular functional form, we also weight our $\widehat{ATT}$ estimator pooling taking into account the estimator precision, although we assume a linear fitting. We show in Figure S11A the non-pooled ATT estimates for Conifers (just like Fig S5) and an OLS fit (Eq 9) in S11B using a similar jackknife approach as in the RR estimates. We use these ATT estimates in our simulations to calculate the causal change in severity due to the treatment.

$$\widehat{ATT}(a,t) = \alpha + \beta \cdot t + \varepsilon_i \tag{9}$$

To calculate the variances of the $\widehat{ATT}$ defined in 6, we derivate an expression for the variance using M-estimation:

$$\mathbb{V}(\widehat{ATT}(a,t)) = \frac{1}{n_t^2}\left[\sum_{i=1}^{N_t}(Y_{i,a,t} - \mu_{1,i,t})^2 - \sum_{i=1}^{N_c}\omega_{i,a}^2(Y_{i,a,t} - \mu_{0,i,t})^2\right] \tag{10}$$

where μ_1 and μ_0 correspond to the weighted sample mean for both treatment and control, respectively. Notice from 6, μ_0 is the unweighted sample mean of the treatment. These variances are used as weights in 9 to take into account the differences in treatment and control compositions of each focal year. While

a bootstrap approach is also possible giving less conservative estimators of the variance, estimating ω_i is computationally harder in our setting [19]. Results are robust to alternate approaches to pooling estimates at each lag (t), including using a simple averaging that computes the weighted average effects separately in each year using the number of control pixels as weights, and a unweighted least-squares fit to the lag estimates (Fig S19)

S2.4 Spillover estimation

To calculate the spillover effects of wildfire exposure in our sample, we re-define treatments as a function of proximity to a wildfire boundary. Figure 3 shows an example of this approach with the 2020 August Fire, depicting different distances to the boundary from 2 km to 15 km. To calculate spillovers, we define treated units as pixels at different distances from pixels that burned at low severity. Following the same approach for the direct exposure, we calculate a set of weights $\omega_{i,a}$ for each focal year (a) and calculate both causal estimators: the average change in severity ($\widehat{ATT}(a,t)$) and the risk ratio of the treatment ($\widehat{RR}(a,t)$).

One possible concern with this distance-based identification strategy is that observed fires boundaries could reflect various factors (e.g the presence of roads, or amplified suppression effort near communities) that would also shape subsequent burn risk in nearby areas. To reduce the importance of these potential unobserved factors, we restrict our sample to "remote" fires that are further from human activity, which we define as wildfires that within 10 kilometers of their boundary are below the median of the state population density (Fig S6A), using spatially interpolated population census data from the Gridded Population of the Word (V4) dataset [10] between 2005 and 2015. This leaves us with an effective sample of 943 wildfires, all comparable in terms of acreage (t-test on difference in means: $t = -0.74$; $p > 0.5$) and severity ($t = -1.70$; $p > 0.05$) with the full MTBS sample. To consider possible migration patterns or inherent changes in population structure within our analysis time frame, we use the closest census estimate to the wildfire start year when applying this population density filter.

Since these estimates are also used in our simulation of prescribed burning where treatments are smaller, an additional concern is that we will overestimate spillovers if typically larger low-severity wildfires are more limiting than smaller prescribed fires. To address this concerns as best we can in available data, we use the same pipeline described but limit the sample to wildfires below the 25-percentile ($< 4{,}000$ acres) of burned acreage in our remote fire sample. We show that our main spillover estimates still largely hold in this sample of smaller fires, although estimates are somewhat noisier given smaller sample sizes (Fig S12).

S2.5 Covariates including in balancing

Weather Monthly means, minimums, and maximums of surface temperature, rainfall, vapor pressure deficit (VPD), and dew-point for each pixel are derived from PRISM [12]. This product calculates daily estimates for these variables at a 4 km^2 resolution from the continental United States. We are particularly interested in rainfall and VPD have given their singular influence over fire vulnerability. Increases of the latter are associated with an increase in burned area, particularly in areas where vegetation is water-limited [18, 21, 22]

Vegetation We use fractional vegetation cover at a 30-meter resolution in California from 1985 to 2021 [23] to calculate the proportion of different vegetation types per each pixel in our 1 km^2. We use these to capture within-pixel vegetation cover variations across time that can influence fire through fuel availability.

Disturbances To compare pixels with similar disturbances and fire experiences, we use data from the Fire Information for Resources Management System (FIRMS) from March 2000 to 2021. In particular, we use the Fire Radiative Power (FRP) captured by MODIS Terra (`MOD09GA`) and Aqua (`MYD09GA`) collections to capture the fire intensity history for each 1 km^2 pixel in our dataset. We calculate the monthly maximum FRP for the balancing period using the maximum measurement per each day over for each pixel.

Additionally, we use a vegetation disturbances database at a 30-meter resolution in California from 1984 and 2021 [24] which measures different vegetation disturbances (i.e. browning or tree mortality). Fires can drive structural changes in vegetation as areas as constantly exposed to wildfires, thus accounting for these changes is important for a balancing strategy.

Physical attributes We use a global standardized elevation model [4] as an input to calculate slope and elevation at a 1 km^2 resolution, using Python's `xarray-spatial` slope algorithm.

S3 Simulating the air quality benefits of a prescribed fire policy

To estimate the potential costs and benefits of a prescribed fire policy for air quality, we build a simple model that compares the air quality impacts of the wildfires that occurred between 2010-2020, to what we estimate would have happened had a given prescribed burn policy been enacted over that period. The difference between these two scenarios depends on a number of key parameters, including: the number of pixels treated with low severity fire under the policy; the reduction in future fire severity achieved by an initial low severity treatment, which includes the probability that an initial treated pixel actual burns in a subsequent wildfire; the smoke emitted from low-severity treatments and the reduction in smoke during subsequent wildfires resulting from any changes to fire severity.

A two period model of prescribed fire treatments Consider the simplest setting with two periods: $\tau - 1$ when the prescribed fire policy is enacted and its costs (in terms of emitted smoke) are realized, and period τ, the after-treatment period where wildfires occur and any benefits of reduced wildfire severity and reductions in emitted smoke are realized. In $\tau - 1$, our simulation randomly allocates a given number of pixels $Rx_{\tau-1}$ to be treated by prescribed fire; these are pixels where no treatment or wildfire had happened previously in our sample period (See Fig S8). This implies that a pixel can only be treated once during the simulation.

We calculate the "cost" of this treatment as the change in surface concentration of smoke $PM_{2.5}$ resulting from the treatments. To estimate this cost, we match each of k fires in the MTBS database (our primary sample) to the set of fires studied in an earlier analysis that attributed observed smoke PM2.5 concentrations to individual fires [25], successfully matching 488 (or 64.2%) of the wildfires in the MTBS dataset over the 2006-2020 period. The matched sample is representative of the overall distribution of ΔNBR in California for the 2000-2021 period (Figure S9B), and includes 45 large prescribed fires. We then flexibly estimate the relationship between average burn severity and attributed smoke at the fire level, controlling for fire size and the number of days over which each fire burned ($\boldsymbol{X}_k$), and additionally for a set of year fixed effects (δ_t) that accounts for state-wide annual trends in burn severity and smoke $PM_{2.5}$:

$$PM_{2.5_{k,t}} = \delta_\tau + f\left(\Delta NBR_{k,t}\right) + \gamma \boldsymbol{X}_k + \varepsilon_{k,t} \tag{11}$$

The outcome $PM_{2.5_{k,t}}$ is defined by [25] as the cumulative effect of fire k on surface-level smoke PM concentrations, which is calculated in that paper as the product of the number of days a given pixel was affected by smoke from that fire multiplied by the smoke concentration on affected days, summed over

affected pixels. As argued by [25], this integrated measure of smoke exposure is a good proxy for health impacts so long as a given health outcome of interest is linear in smoke exposure; that study provides evidence that many such outcomes appear to be linear. "Linearity" here is equivalent to assuming that a fire that raises surface concentrations for $10^{\mu g}/_{m^3}$ on two days is twice as harmful as a fire that raises concentrations by $10^{\mu g}/_{m^3}$ for one day, that a fire that raises surface concentrations for $10^{\mu g}/_{m^3}$ on two pixels for a day is twice as bad as a fire that raises concentrations by $10^{\mu g}/_{m^3}$ for one pixel, and that a fire that raises surface concentrations by $5^{\mu g}/_{m^3}$ on two pixels for a day is equivalently harmful to a fire that raises concentrations by $10^{\mu g}/_{m^3}$ for one pixel.

We fit $f(\cdot)$ using polynomials of order $d \in \{1, \cdots, 9\}$. To avoid over-fitting, we sample a 80-20 train-test split of our data and pick the best polynomial fit using the lowest RMSE as the evaluation metric. Fig S9A shows the best fit, which happens to be the linear model. Denote $f_{PM_{2.5}}$ the linear estimate shown in Fig S9A, which maps changes in burn severity to changes in surface smoke concentration.

Denote $\underline{\Delta \text{NBR}}$ as the average treatment severity from prescribed fire treatments, which we estimate as a range of ΔNBR between 45 and 100 from our matched MTBS sample that includes 45 prescribed fires. We then calculate the summed cost of the prescribed fire treatment in terms of the smoke it generates:

$$C_{\tau-1} = f_{PM_{2.5}}\left(Rx_{\tau-1} \times \underline{\Delta \text{NBR}}\right) \tag{12}$$

To calculate the subsequent benefits of this treatment in terms of reduced smoke, we track treated pixels in the post-treatment period (τ), during which pixels either don't burn in subsequent wildfire or burn at observed severity $\Delta NBR_{i,\tau}$ (i.e. at the severity values we observe in the MTBS data). When pixels are observed to burn, we adjust observed severity based on whether pixel i happened to be treated in the previous period, using our ATT estimates of the impact of low severity treatments on future severity, which here we denote $\beta_{\tau}^{\Delta NBR}$. To capture uncertainty in these treatment effects, we sample from the distribution of the estimator given by $\beta_{\tau}^{\Delta NBR} \sim \mathcal{N}(\beta, \widehat{SE}_{\hat{\beta}})$. We then calculate the pixel-level (i) change in the observed severity $\Delta NBR_{i,\tau}$ as a result of any treatments that occurred in the previous period.

$$\Delta NBR_{i,\tau}^{Rx} = \Delta NBR_{i,\tau} + \beta_{\tau}^{\Delta NBR} \times \mathbb{1}_{Rx_i} \times \mathbb{1}_{F_i} \tag{13}$$

where $\mathbb{1}_{Rx_i}$ is an indicator for whether pixel i was treated with prescribed fire, and $\mathbb{1}_{F_i}$ is whether pixel i subsequently burned in a wildfire. This equation makes clear that the benefit of reduced fire severity $\beta_{\tau}^{\Delta NBR}$ is only realized if the pixel is both treated and is exposed to subsequent wildfire. If the pixel is not treated or is treated and has no subsequent wildfire exposure, then it will keep the observed $\Delta NBR_{i,\tau}$ value.

To model the spillover benefits from prescribed fires, we add an additional term to Equation 13 to capture the spillover:

$$\Delta NBR_{i,\tau}^{Rx} = \Delta NBR_{i,\tau} + \underbrace{\beta_{\tau}^{\Delta NBR} \times \mathbb{1}_{Rx_i} \times \mathbb{1}_{F_i}}_{\text{direct effect}} + \underbrace{\delta_{\tau}^{\Delta NBR} \times \mathbb{1}_{Rx_i} \times \mathbb{1}_{F_i} \times S_i}_{\text{spillover effect}} \tag{14}$$

where S_i is the number of nearby spillover pixels affected for every burned pixel. Our main spillover results suggest that reductions in burn severity are observed up to 5 km from a fire boundary. Thus for every 1 km pixel treated, S_i is 24 under a 2 km spillover - i.e. 24 pixels around the treated pixel get benefits $\delta_{\tau}^{\Delta NBR}$). In practice, at higher treatment levels, S_i is substantially less than 24 under a 2 km spillover, as most of CA forest receives treatment after a decade of large annual treatments (see below).

For every treated pixel that happened to be treated in observed fire k, we then aggregate Equation 13 or 14 to the fire level, such that we get the total sum of severity for a particular fire k:

$$\Delta NBR^{Rx}_{k,\tau} = \sum_{i \in k} \Delta NBR^{Rx}_{i,\tau} \tag{15}$$

Finally, to calculate benefits (B^{Rx}_{τ}) in terms of changes in surface smoke $PM_{2.5}$, we use the above-estimated $f_{PM_{2.5}}(\cdot)$ to translate changes in fire specific severity to fire specific total contributed smoke. For each fire k, we estimate the smoke that occurred under observed severity ($f_{PM_{2.5}}(\Delta NBR_{k,\tau})$) as compared to the smoke that would have occurred had at least some pixels been treated in the perimeter of fire k prior to k having burned ($f_{PM_{2.5}}(\Delta NBR^{Rx}_{k,\tau})$). These can be identical if there are no prescribed fire treatment areas in a particular wildfire; in this case the benefits from treatment will be zero. We aggregate across all fires in CA in a given year τ to arrive at total $PM_{2.5}$ benefits:

$$B_{\tau} = \sum_{k} f_{PM_{2.5}}(\Delta NBR_{k,\tau}) - f_{PM_{2.5}}(\Delta NBR^{Rx}_{k,\tau}) \tag{16}$$

These smoke benefits can then be compared to the smoke costs defined in Equation 12, for instance (as below) by taking the ratio of cumulative smoke reductions (benefits) to initial smoke costs. We note that if $f_{PM_{2.5}}()$ is linear, then the benefit-cost ratio of prescribed burning, in terms of smoke reduction, is simply the ratio of the reduction in wildfire severity from burning to the increase in severity from the prescribed burn itself.

Aggregating benefits across treatment years As calculated above, treatment benefits depend on the observed wildfire history, with treatments having larger benefits in high fire years. The probability of fire can vary substantially across years; in our data we calculate that in California conifer forests, the probability any pixel burned in 2020 was 20.13% as compared to 0.6% in 2010. To ensure that our estimates of the time path of benefits of prescribed fire treatments do not depend on the specific sequence of fire years in our observed data, we run our simulation multiple times, each time using a different start year. This ensures that our estimated benefit two years after treatment is the expected value of the benefits in year two, given the range of possible fire years that could have occurred two years after a given start year in our data. Specifically, for each year starting in 2010 and going through 2020, we start a treatment simulation as described above (Fig S8), calculating benefits in every available subsequent period until the end of our simulation in 2021. Thus for the first year in 2010, we will calculate treatment benefits for the eleven subsequent years following treatments that begin in 2010; denote benefits in each year in this setting as B^1_{2010}, B^1_{2010}, ... B^{11}_{2010}. For treatments that begin in 2020, we can only calculate the benefits B^1_{2020} for the immediate year after treatment is begun (2021). Benefits estimated in each simulation can be summarized in the matrix B_{Rx} (Eq 17) where each row represents a simulation beginning in the subscript year and each column is a period relative to the treatment (column 1 is first year of treatment, column 2 the second year, and so on). In our experiment, our matrix has a size of 10 rows by 11 columns.

$$B_{Rx} = \begin{bmatrix} B^1_{2010} & B^2_{2010} & \cdots & B^{10}_{2010} & B^{11}_{2010} \\ B^1_{2011} & B^2_{2011} & \cdots & B^{10}_{2011} & NA \\ B^1_{2012} & B^2_{2012} & \cdots & NA & NA \\ \vdots & \vdots & \cdots & \vdots & NA \\ B^1_{2020} & NA & \cdots & NA & NA \end{bmatrix} \tag{17}$$

To estimate the average benefit a policy would generate in the years following treatment, we then average all the benefits for each period relative to the treatment across different start years, i.e. take the column average of our benefits matrix, yielding the average benefits sequence for all the periods relative to the treatment: $\{B_{Rx}^{\tau+1}, B_{Rx}^{\tau+2}, \ldots, B_{Rx}^{\tau+11}\}$.

We then calculate the ratio of cumulative benefits to costs in year T after treatment $\tau = 0$ as:

$$\text{Net Benefit}_{\tau} = \frac{\sum_{\tau=0}^{T} \frac{1}{(1+\delta)^{\tau}} B_{Rx}^{\tau}}{C_{\tau-1}} \tag{18}$$

where δ is the discount rate, which we vary from 2% to 10%, the latter representing a "political" discount rate for a policymaker with a preference for policies that pay out quickly. Estimates of Equation 18 are reported in Fig 4 under different discount rates and with and without spillovers, and represent the ratio of discounted expected cumulative smoke benefits to initial smoke costs of treating an acre of conifers in California with prescribed fire.

Uncertainty quantification To quantify total uncertainty in cumulative net benefits estimated in Equation 18, we incorporate two possible sources of uncertainty on each of our simulation runs (1,000 runs in total). First, we randomly allocate treatments, drawing pixels without replacement from the universe of conifer forests in California to take into account the treatment location uncertainty. We also draw without replacement across treatment years to avoid treating the same place more than once in our experiment. Second, for each realization of treatment locations, we use a different draw of the $\beta_{\tau}^{\Delta NBR}$ parameter, such that we capture the treatment effect uncertainty. Finally, we show the average net benefit of treatment of all the treatment years in Fig 4 under different discount factors (δ) with the uncertainty estimations defined above. We note that we do not propagate uncertainty in estimates of $f_{PM_{2.5}}(\cdot)$, given that any linear estimate of the function will show up in both the numerator and denominator of the net benefit ratios we report, and thus cancel.

Spillover estimation To estimate spillover benefits, we first define the size of the spillover that determines S_i in Equation 14. Following the results in Figure 3, we conservatively assume that spillovers are only present within 2 km of the treatment. This implies that for each 1 km^2 area directly treated with fire, an additional 24 km^2 ($S_i = 24$) receive "spillover" treatments. However, because we restrict our simulation to only apply treatments to pixels who have not experienced any previous treatment (direct or spillover), we do not re-treat pixels within the 2 km^2 buffer that have already experienced either direct or spillover treatment. As total treated area grows across our decade-long simulation, this implies that S_i in practice decreases substantially over time (Fig S13), consistent with a real-world setting in which most areas have already received treatment after a decade of high annual treatments. This is depicted in Fig S21. On average S_i ranges from an initial value of 24 down to 7 by the end of a decade, under annual treatments of 2,000 km^2 (500,000 acres/year).

Quantifying changes in state smoke concentrations To calculate the reduction in overall wildfire smoke under different policy scenarios at the state level, we calculate the ratio between the predicted smoke concentrations under the observed severity and the predicted concentrations for each simulated treatment, taking into account the increase in smoke from the treatments themselves, the reduction from the impacts of treatments of future fire severity, and that treatments are applied every year and that the effect of one year's treatment persists into future years.

Specifically, for each year of the policy, we calculate the cumulative percent change of the policy since its enactment:

$$\%\Delta\text{Smoke ratio}_{\tau} = \sum_{\tau=2010}^{T} \frac{f_{PM_{2.5}}(Rx_{\tau} \times \underline{\Delta\text{NBR}}) - \left[\sum_k f_{PM_{2.5}}(\Delta NBR_{k,\tau}) - f_{PM_{2.5}}(\Delta NBR_{k,\tau}^{Rx})\right]}{\sum_k f_{PM_{2.5}}(\Delta NBR_{k,\tau})} \quad (19)$$

where the first term in the numerator is the smoke emitted from the treatments in that year and the second term in brackets in the numerator is the benefits from Rx treatments in terms of the reduction in smoke in subsequent wildfires, as calculated in Equation 16. The denominator is the smoke from observed wildfire. The resulting estimate is then the percent increase in cumulative smoke from the prescribed burning policy relative to had the policy not occurred. Results are shown in Fig 5C.

Policy targeting As spatial treatment targeting – i.e. the probability that a pixel treated with low-severity fire is later exposed to wildfire – plays a key role in the realized benefits in Equation 15, we quantify this parameter for both our simulated policies (where pixels are randomly allocated to treatment) and the relatively small number of observed prescribed fire treatments reported by the CalFIRE's Fire and Resource Assessment Program dataset from 2010 to 2021 (1860 total treatments covering $1,189$ km^2). To calculate this parameter we compute the cumulative share of any simulated or observed treatment to encounter a wildfire in the years after treatment. Formally, we count the number of initial treated pixels that later overlapped with a wildfire footprint in year t as ($\mathbb{1}_f^t$) and divide it for the number of treatments $R_x^{t=0}$ in the initial year:

$$S_T = \frac{\sum_{\tau=0}^{T} \mathbb{1}_f^{\tau}}{R_x^{t=0}} \quad (20)$$

In this calculation we only include the dominant and relevant type of prescribed burning: broadcast burning, as this type is the one most comparable to our analysis. Including other types (e.g. Fire Use, Jackpot, or Machine Pile burn) does not change this calculation significantly. We report the average of this cumulative share (S_T) across all the treatment years (2010 - 2020) in Fig S20, such that (for instance) the "2 years after treatment" estimate is the average number of pixels treated in 2010 that burned by 2012, treated in 2011 that burned by 2013, treated in 2012 that burned by 2014, etc. Estimates thus combine low burn probabilities early in the sample with much higher burn probabilities later in the sample (2020 and 2021 in particular).

Supplemental Figures

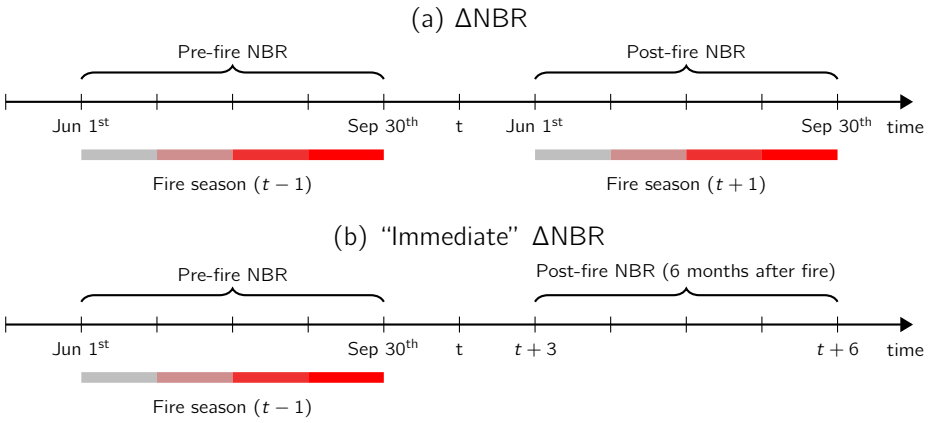

Figure S1: ΔNBR Calculation for a fire occurring in t: We use two strategies to measure ΔNBR following [16]. In the panel **a.** both pre-fire and post-fire periods are measured within the previous and next year's fire season, respectively. In panel**b**, and to capture the severity in vegetation with rapid re-sprouting, we modify the post-fire period to be defined between the next 3-months after the ignition date, through up to 6 months afterwards.

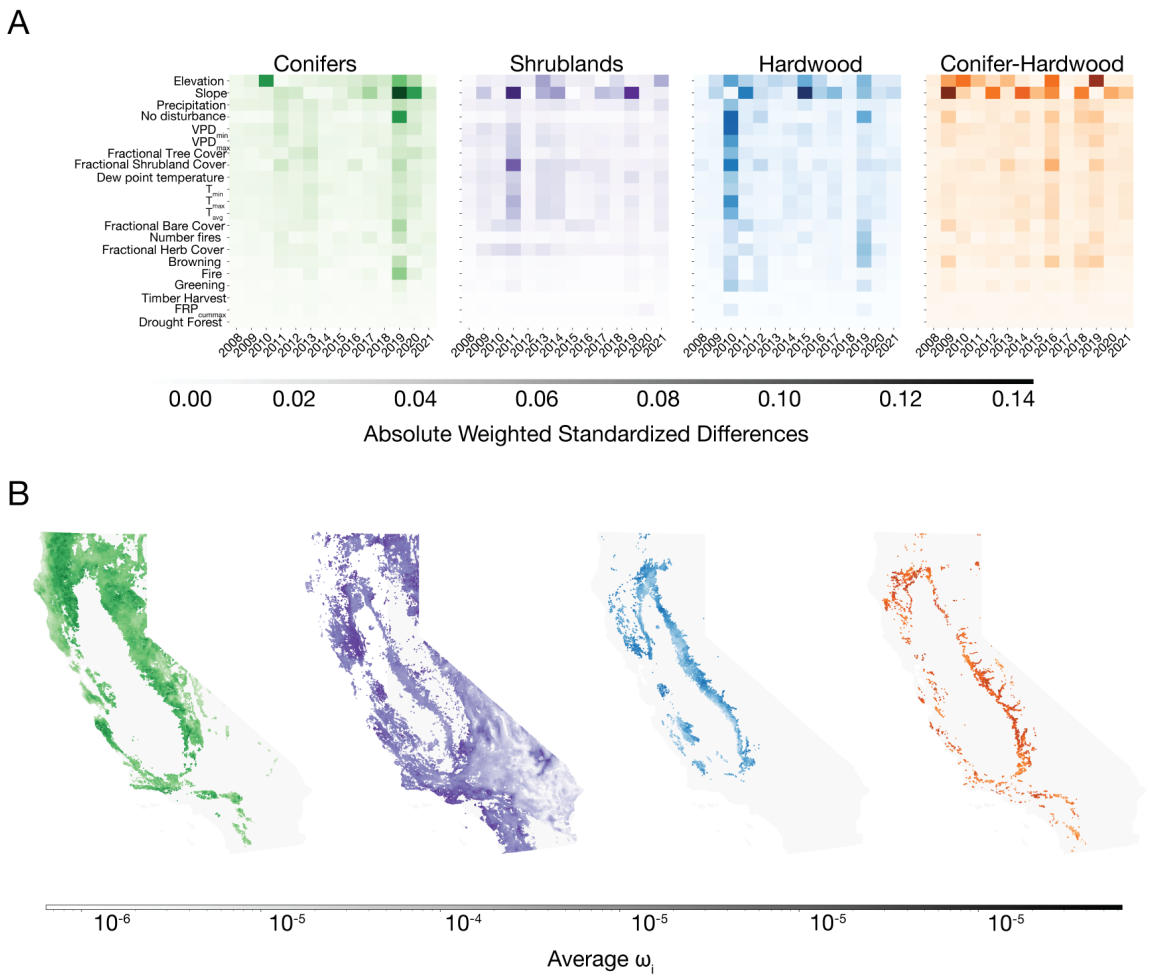

Figure S2: Synthetic control balancing weights. **a.** We calculate the absolute weighted standardized differences (AWSD) for all the covariates used in our covariate balancing strategy for each of the evaluated years and land types. For all the monthly variables, like precipitation, we took the average AWSD to capture the general balance along the time series. Pixel physical attributes have slighter large differences between treatment and control groups, but is still less than 0.2, the standard for RCTs. **b.** Average balancing weight (ω_i) for each land type; colors correspond to categories in A. This is the weight assigned to each control unit on average across all of the focal years (2008 - 2020).

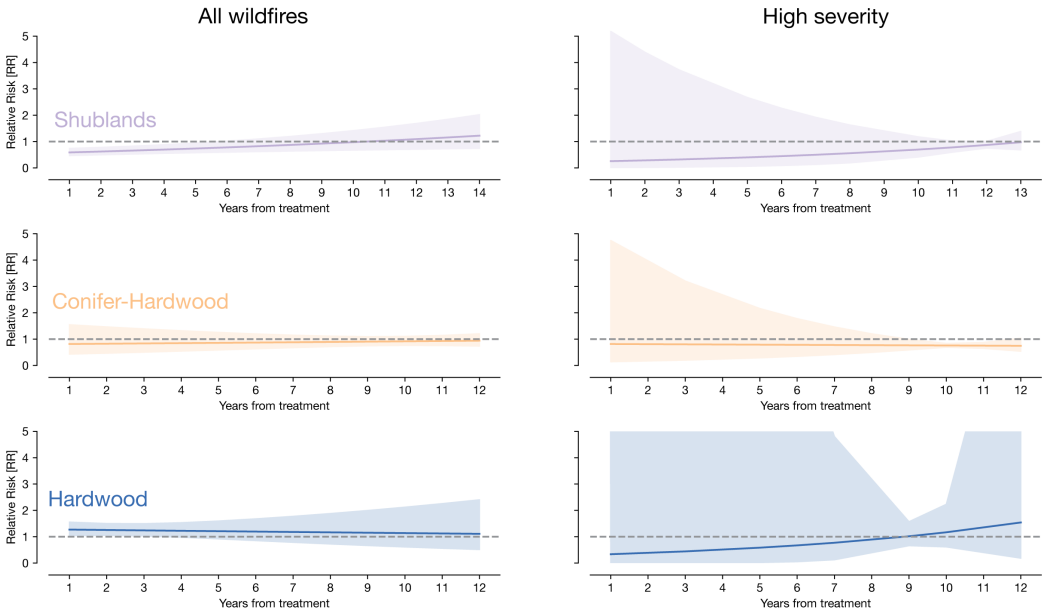

Figure S3: Impact of low severity treatments on subsequent fire risk in non-conifer land types.We explore the effect of the low-severity treatment across non-conifer land cover types in California. Results are mixed for Conifer-Hardwood and Hardwood. For shrublands, we observe an immediate reduction in subsequent risk for all fire types, with an immediate reduction of 42% [95% CI: 53,3 - 25.8], but this effect much noisier when considering impact only on subsequent risk of high severity fire

.

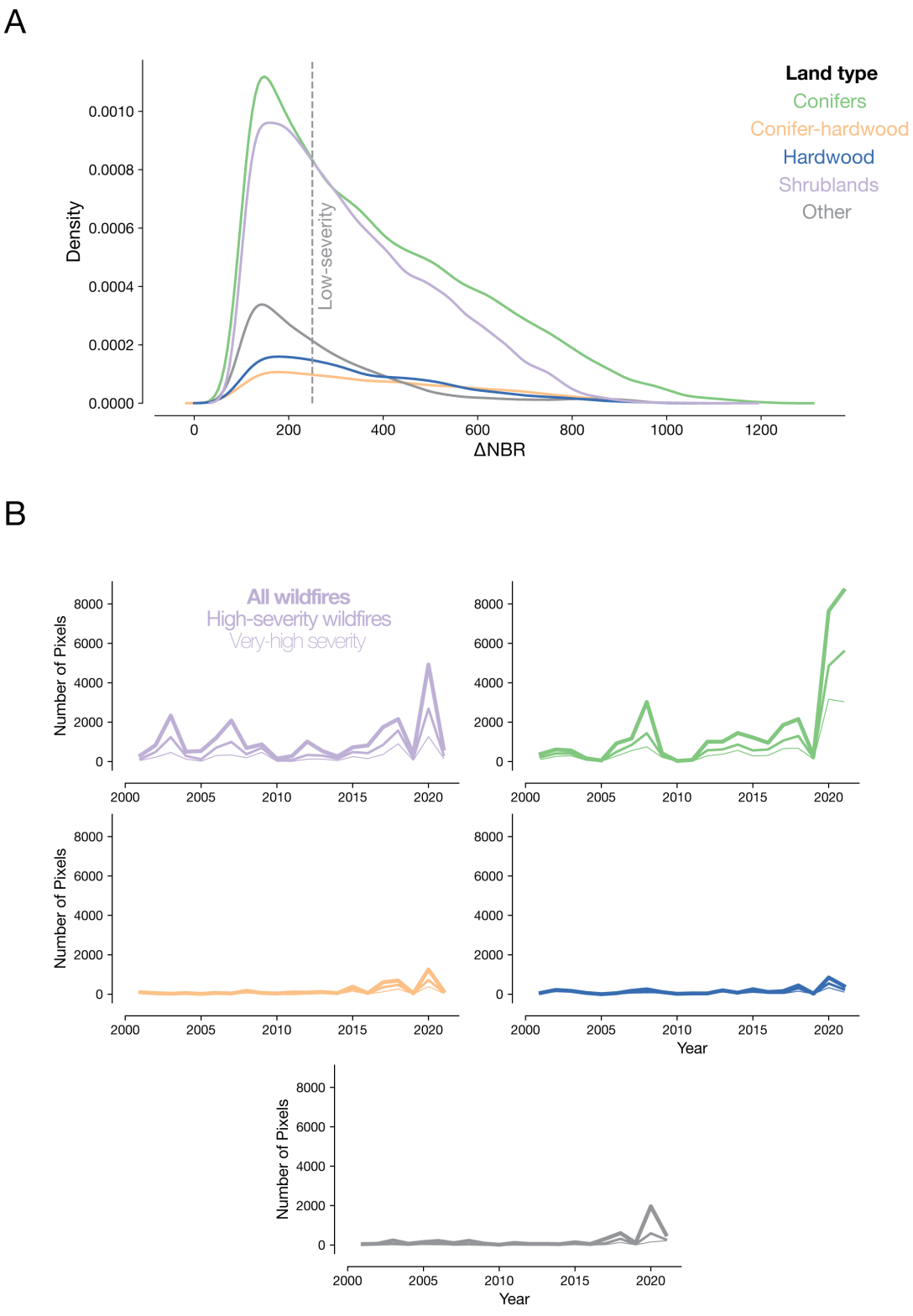

Figure S4: Severity class distribution across land types. **a.** The distribution of positive values of severity across land types for all wildfire events in the MTBS sample from 2000 to 2021. The dotted line is the threshold of low-severity ($0 \leq \Delta NBR < 270$). Conifers and Shurblands are wildfires' dominant vegetation and more than half of the pixels burn at low-severity **b.** Severity timelines for each land type using the same classification we use to define relative risks in the regression results: all wildfires include all detectable severity classes ($\Delta NBR \geq 0$), high-severity ($270 \geq \Delta NBR \geq 660$), and very high-severity ($\Delta NBR \geq 660$). Colors match vegetation types in **a.**.

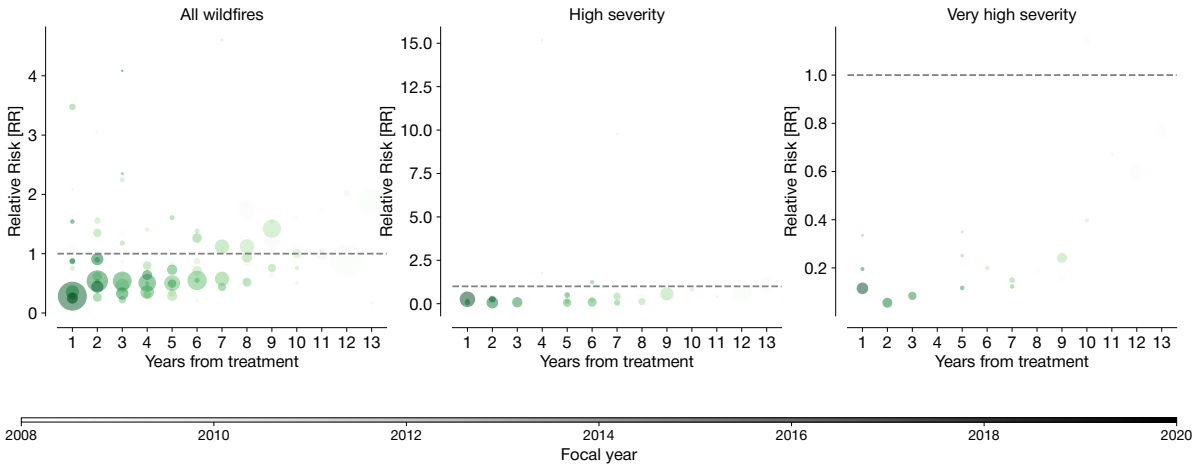

Figure S5: Pooling of Relative Risk estimates: Non-pooled estimates that underlie pooled results reported in Figure 2. Each point represents the raw relative risk (RR) estimates for each focal year and comparison group. The size of the point represents the size of the control group (wildfires, high-severity or very-high severity) in the synthetic control estimates, corresponding to the precision of the individual relative risk estimates. Lighter shaded points represent early years in the sample, while dark points are treatments close to the end of the study sample

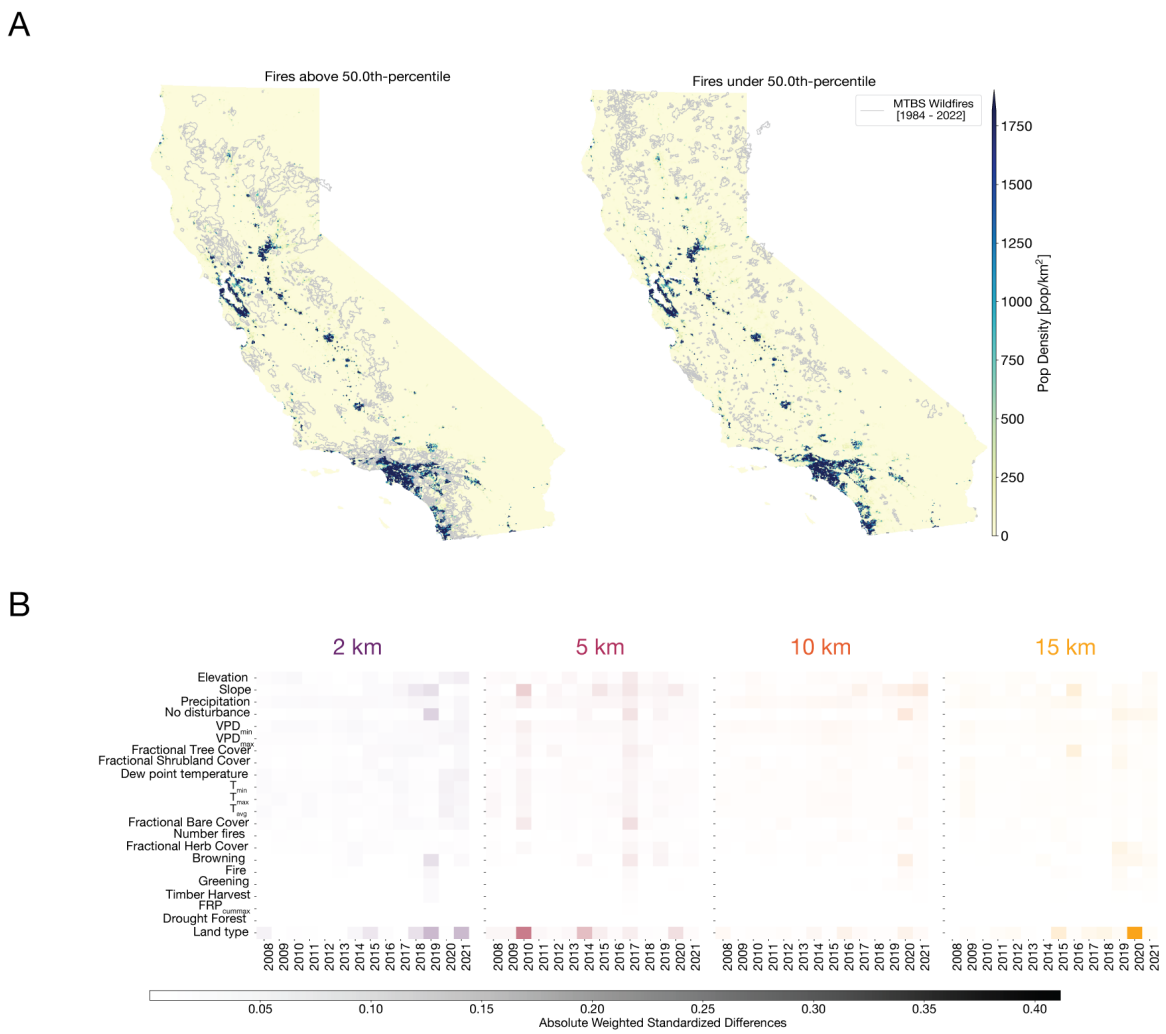

Figure S6: Synthetic control balancing for spillovers: **a.** Shows the population-based inclusion criteria to estimate the MTBS wildfire events spillovers effects. Here we use the [10] Gridded Population of the World (V4) to calculate the population density for each fire in a 10 km buffer around the fire using the closest census year to the year event. We estimate the effects with remote fires only, meaning all the wildfires with populations less than the sample median in the buffer. **b.** Absolute weighted standardized differences for each of the spillover effects at different spillover distances. These values show a robust pre-treatment balance for all years, with the exception of the land type as these estimations are done with all possible land types.

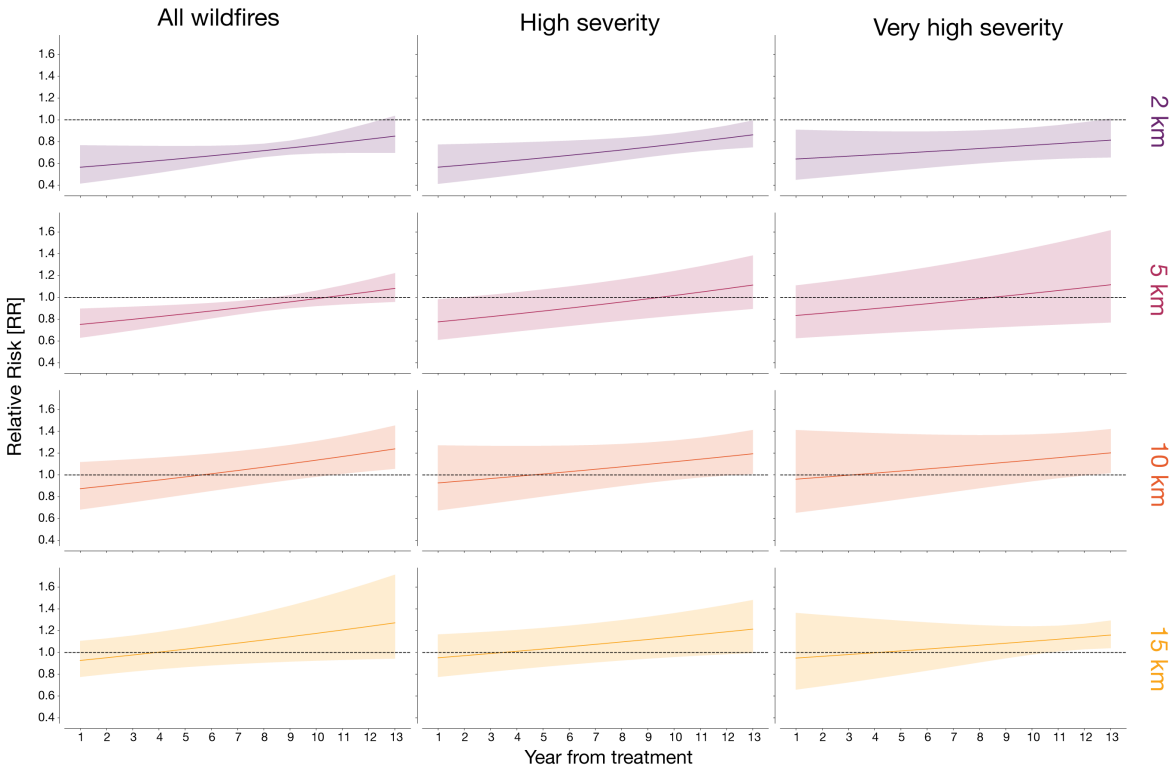

Figure S7: Spillover effects of low-severity fire on subsequent fire risk in nearby unburned pixels, for different fire types and buffer widths. Rows show different distance buffers over which spillover treatments are defined (2 km buffer up to 15 km buffer) and columns show the effect of low-severity fire in a treated pixel on all wildfires or high/ very-high severity wildfires in nearby unburned pixels. As in Figure 3, the limiting effect of previous wildfire burn scars on nearby fire risk is statistically significant and protective against all wildfires, including very high severity ones, within 2 km of the burn scar. This effect decays with distance from the treated pixel, and the large effects over very-high severity is only observed at the immediacy of the burn boundary. The first column is equivalent to the results shown in Fig 3.

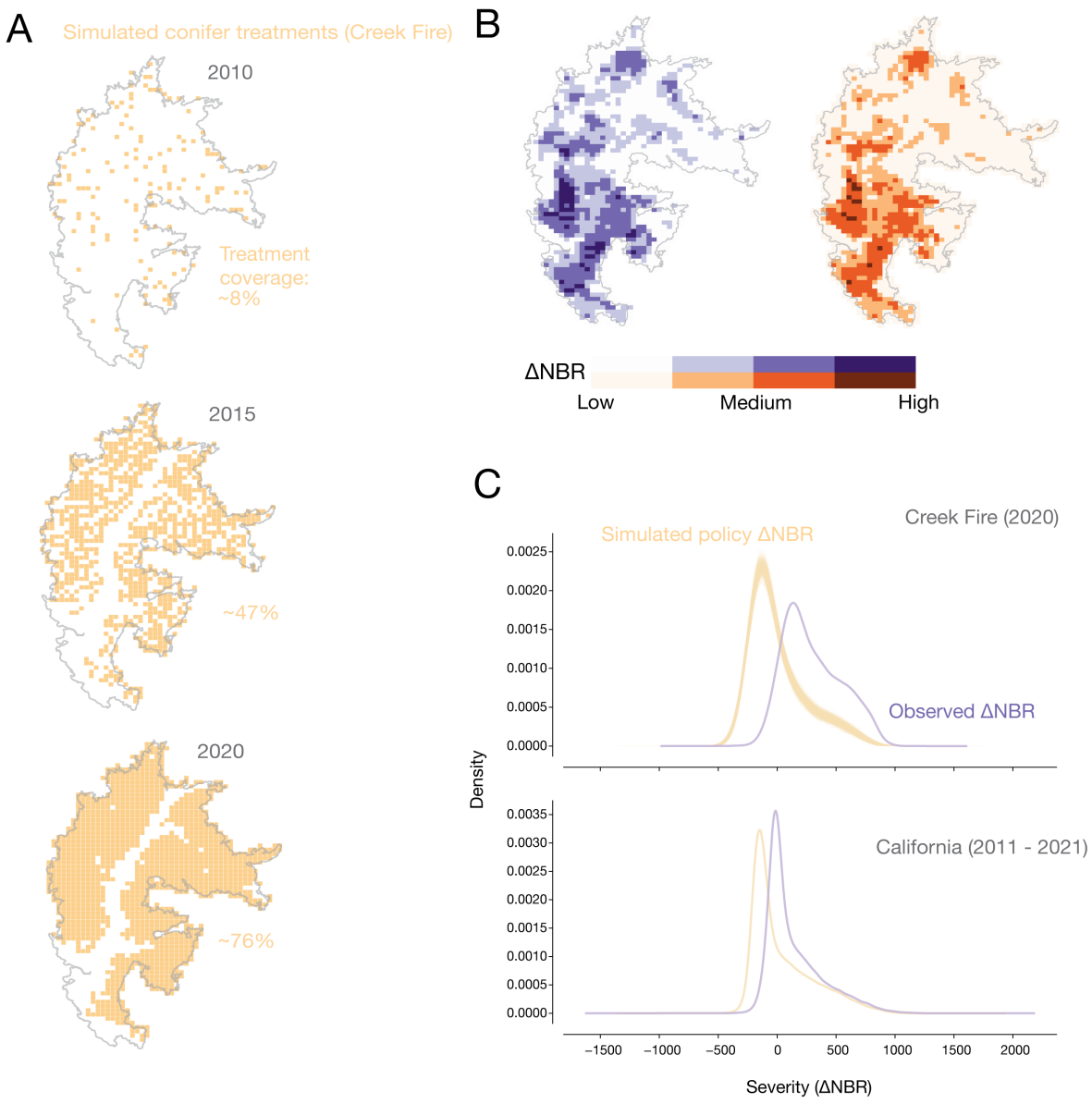

Figure S8: Low-severity treatments simulation: **a.** Example of the coverage of a treatment application (1 M acres) simulation applied to all conifer forest in California starting in 2010, showing treated pixels in the perimeter of the subsequent 2020 Creek Fire. By the last year of treatment in this simulation, the Creek fire has at least 75% of its area covered by previous treatments. **b.** Change in severity classes in the observed data and the simulated data. The effect of the treatment is mostly visible in high-severity areas, where we estimate an average severity reduction of 23.2%. **c.** Distribution of ΔNBR in the observed data compared to the simulation counterfactual in the Creek Fire and across CA as a whole for the 2011 to 2021 period, where each line represents a different simulation run.

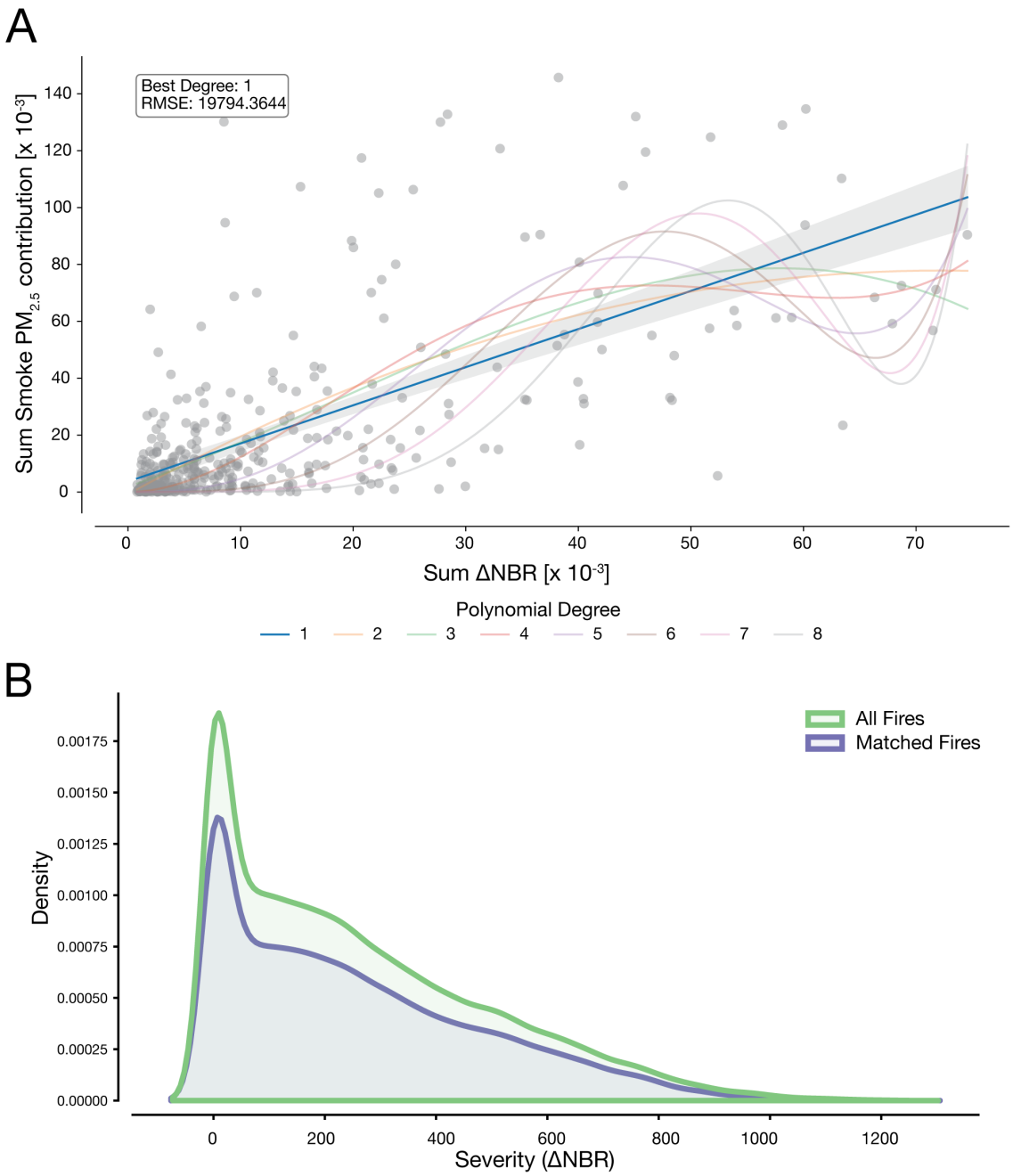

Figure S9: Relationship between fire severity and fire attributed smoke $PM_{2.5}$. **a.** Relationship between the fire-specific attributed smoke particulate matter ($PM_{2.5}$) from [25] and average fire severity, based on large wildfires (> 1,000 ha.) in the MTBS sample from 2006 to 2020 that could be matched to the fires in [25]. Plot shows the fit between the total severity and the attributed smoke $PM_{2.5}$ for different polynomial degrees; the linear model had the lowest RMSE on held out data, and is shown with , 95% confidence interval. **b.** Severity distribution for all matched fires compared to the total number of wildfires in the 2006-2020 period

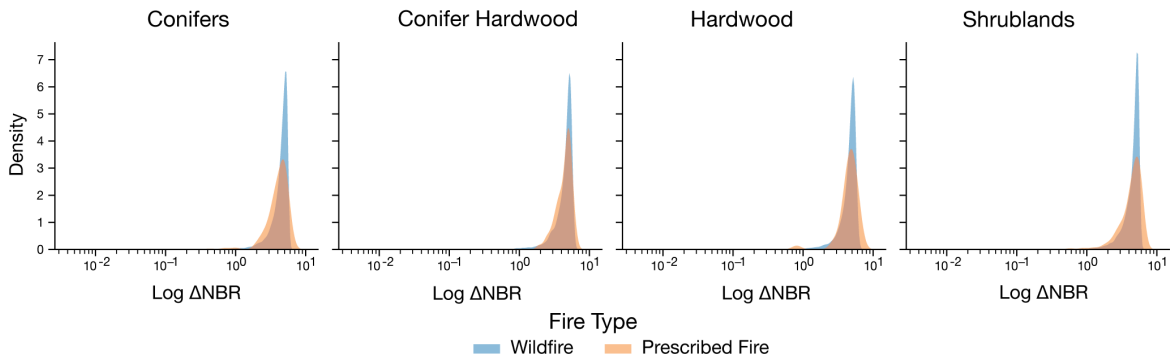

Figure S10: Low-severity wildfires are comparable to prescribed fires in severity. Using the limited set of prescribed fires reported in the MTBS dataset, we compare the severity distribution of these fire treatments against the low-severity wildfires in our sample from 2000 to 2021. We found that the two samples along the threshold of low-severity supporting the hypothesis of low-severity treatments as a valid proxy to fire treatments across different land types.

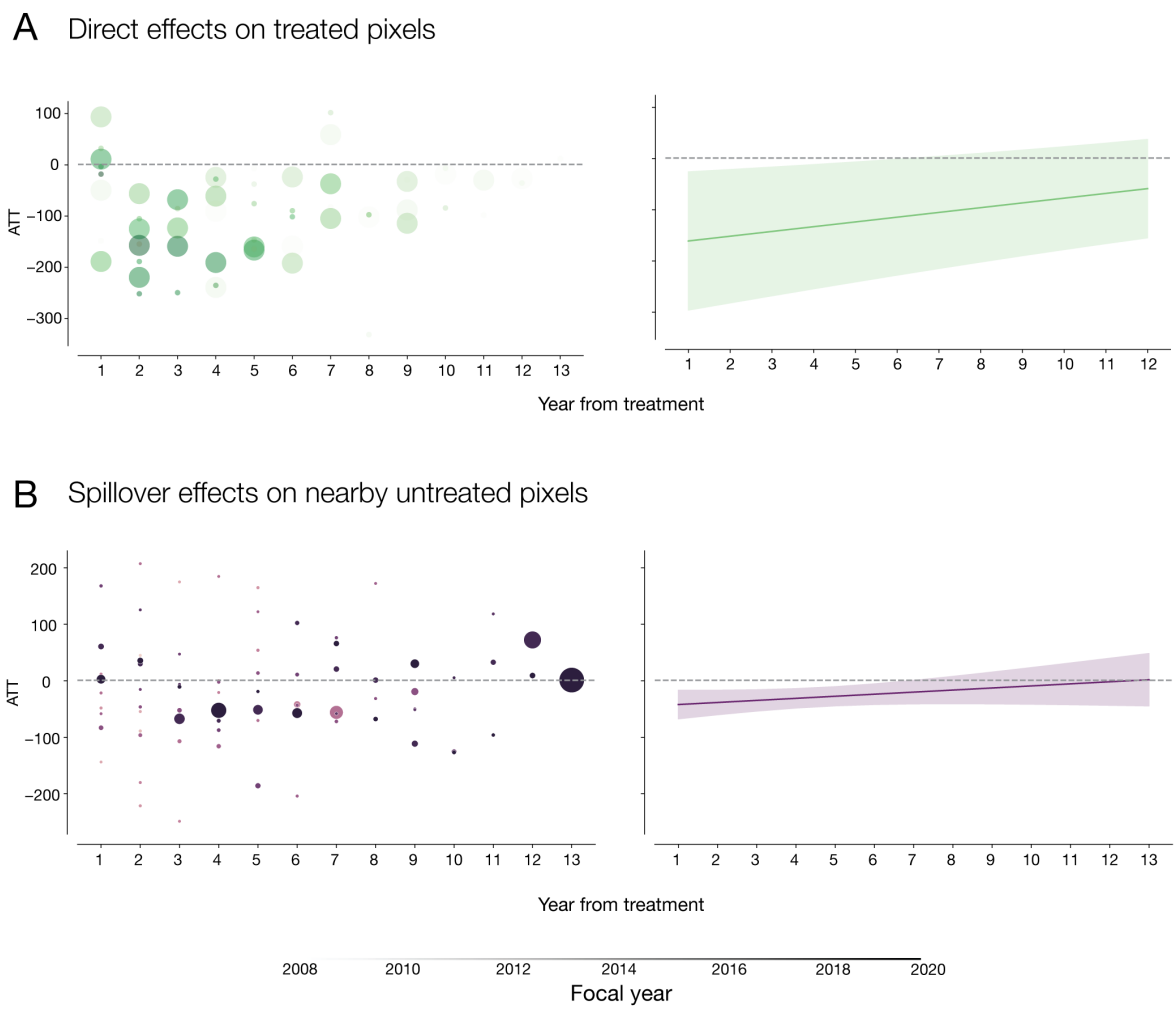

Figure S11: Average change in severity of the direct and spillover exposure to wildfire: Just as Figure 2, we estimate the effect of low-severity treatments on the average reduction of future wildfires. Rather than calculating the change in relative risk of high-severity or very-high severity, we quantify the total change on average severity (ΔNBR) after the exposure using the ATT estimator. For both panels we pool individual estimates using the variance weighted linear fit of the estimates across the lags [Methods SI]. We represent the variance of each un-pooled ATT estimate using the point size, where larger points represent more precise estimates; **a.** shows the non-pooled and pooled results of the effect of low-severity fire on subsequent fire severity on conifers by focal year **b.** shows the same but for the spillover effects.

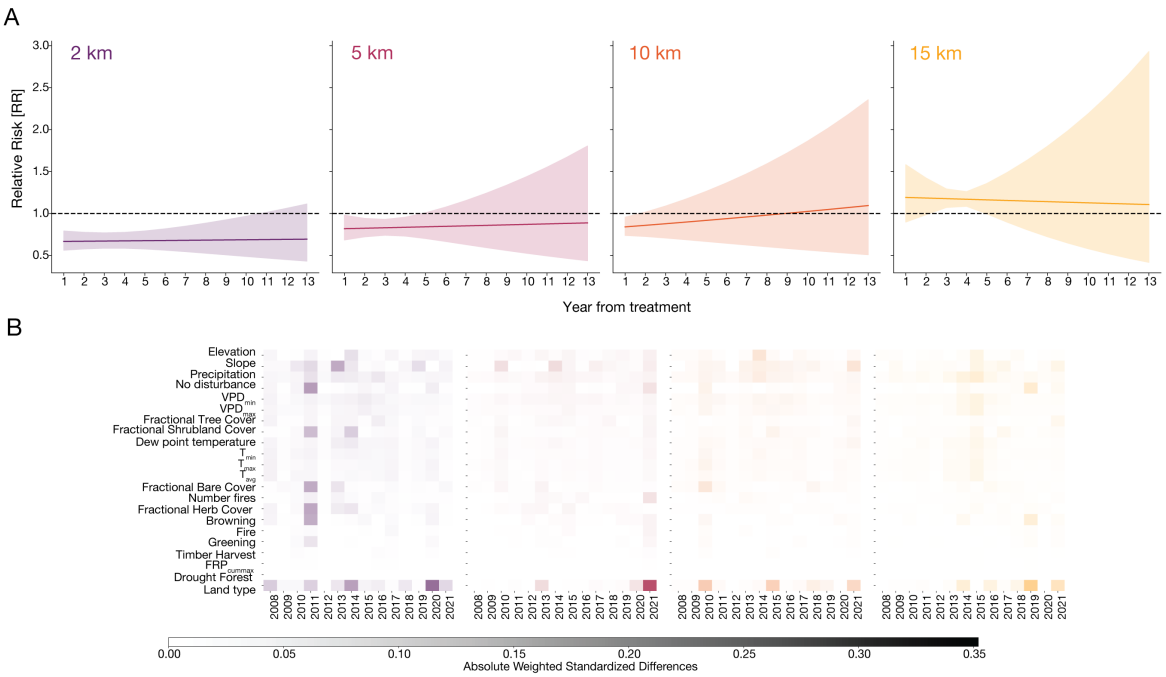

Figure S12: Small wildfires ($< 4,000$ acres) reduce subsequent fire risk in surrounding unburned areas: **a.** We replicate the results shown in Figure 3 using only the fires under the median of the total burned acreage from our sample of remote fires ($x_{med} \approx 4,000$ acres). Compared to the full sample, the spillover (or "shadow") effects of small wildfires are slightly smaller that for larger fires (33.2 % [CI 95%: 20.8% - 43.7%]) but still significant for 9 years within 2 km of the wildfire. For larger distances the effect either vanishes or is close to zero. This shows that even in small burned areas, we can observe the limiting effect of wildfires. **b.** We show the AWSD for the estimates in panel a, with our SC method again balancing covariates successfully across different treatment years.

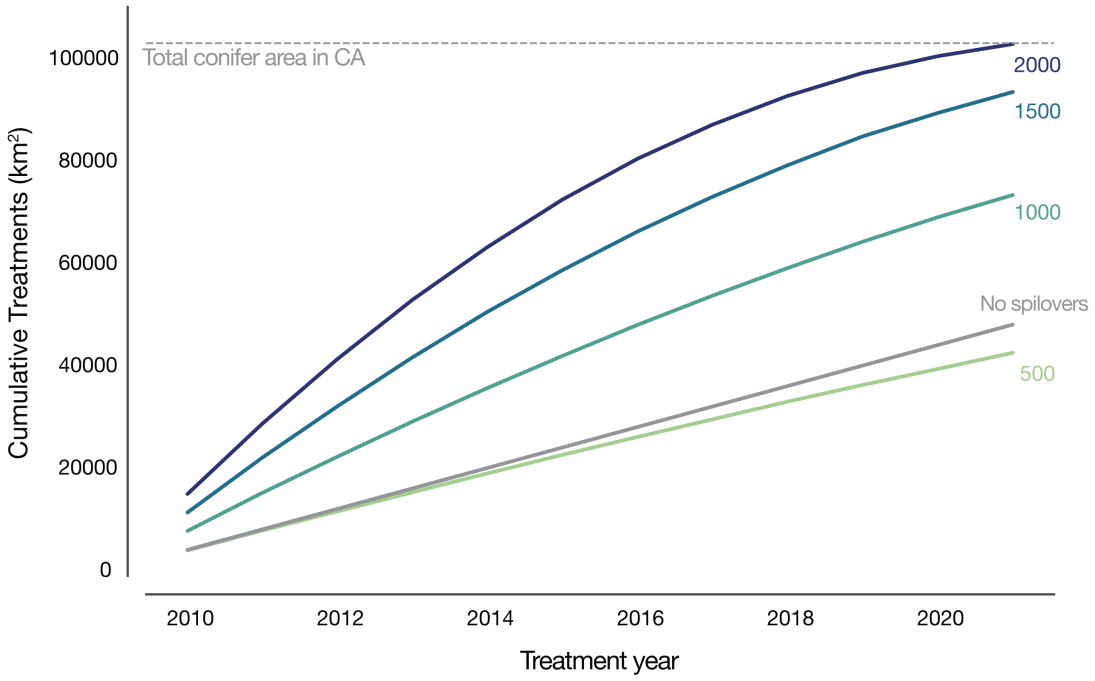

Figure S13: Limits to prescribed fire treatments with spillovers ($\leq$ 2 km): We calculate the total number of available treatments in our simulations with spillovers under the restriction of no re-burning for any treated pixel (Methods SI). We see that treating 500 km^2 with 2 km spillovers is almost equivalent to treating 4,000 acres each year. As we increase the number of treatments, the number of cumulative treated area increases almost linearly, until converging to the total of conifer areas in California. Notice that the no re-burning restriction creates a non-linear behavior in the number of treatments as with an increase of the treatments the sample of available conifers to burn is smaller, so it converges almost logarithmically to the total number of conifers. We see that as a result, this alters the benefits under different number of treatments with a fixed spillover distance as seen in Figure S14.

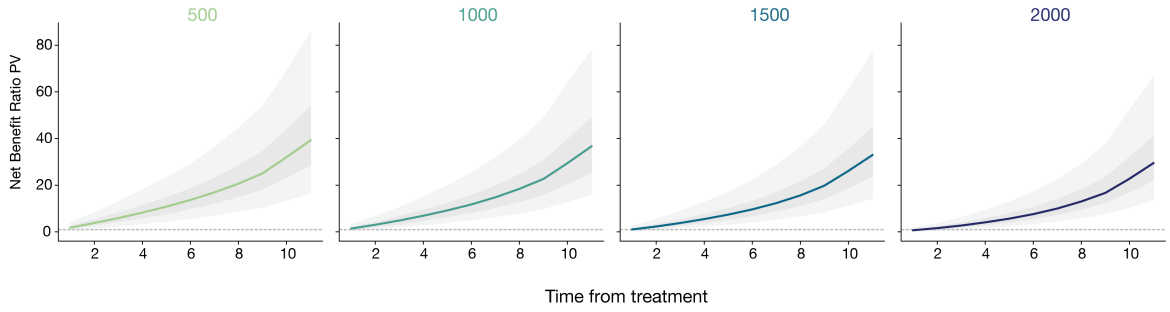

Figure S14: Emissions Net Benefit ratios by spillover treatments: We show the same exercise as Figure 4 using a fixed spillover distance ($\leq$ 2 km) and a 2% discount factor under different treatment sizes. Each panel uses a different number of treatments from 500 to 2,000 ($\approx$ 500,000 acres) with a fixed number of spillovers. The 2,000 treatment size would almost treat every pixel classified as conifer in the state, and would run out of treatments in 10 years, thus the reduction in the benefit-cost ratio compared to other treatment sizes where treatments can be realized.

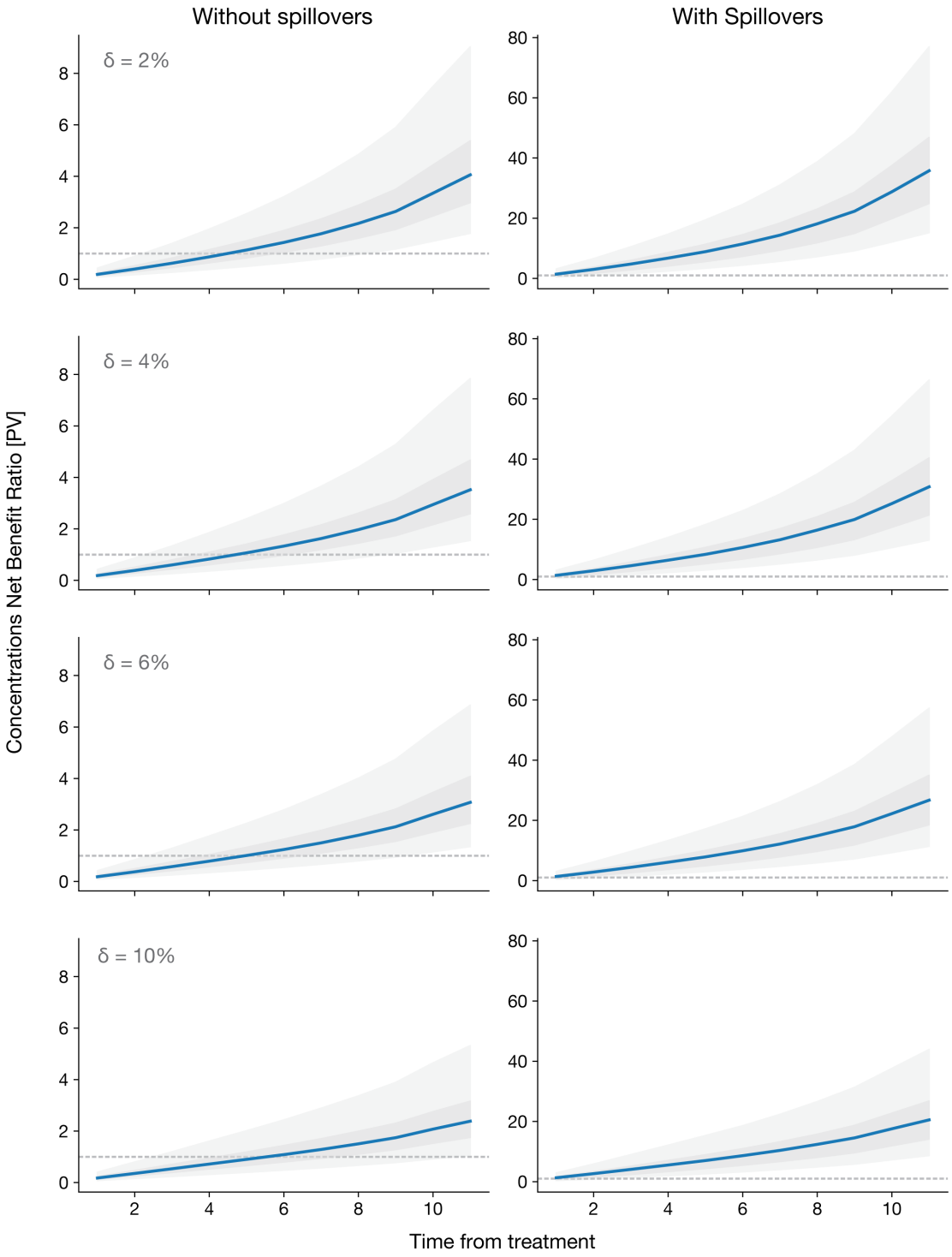

Figure S15: Benefit cost ratio for different discount rates: Just as Figure 4, we show the cumulative present value discounted benefit-cost ratio for a prescribed fire policy under different discount factors. The left panel of the figure shows the ratio of the treatment of 1 million acres/year without considering any spillovers. The right columns shows the benefit-cost ratio of a 500 kilometer/year (124,000 acres/year) with spillover effects up to 2 km^2.

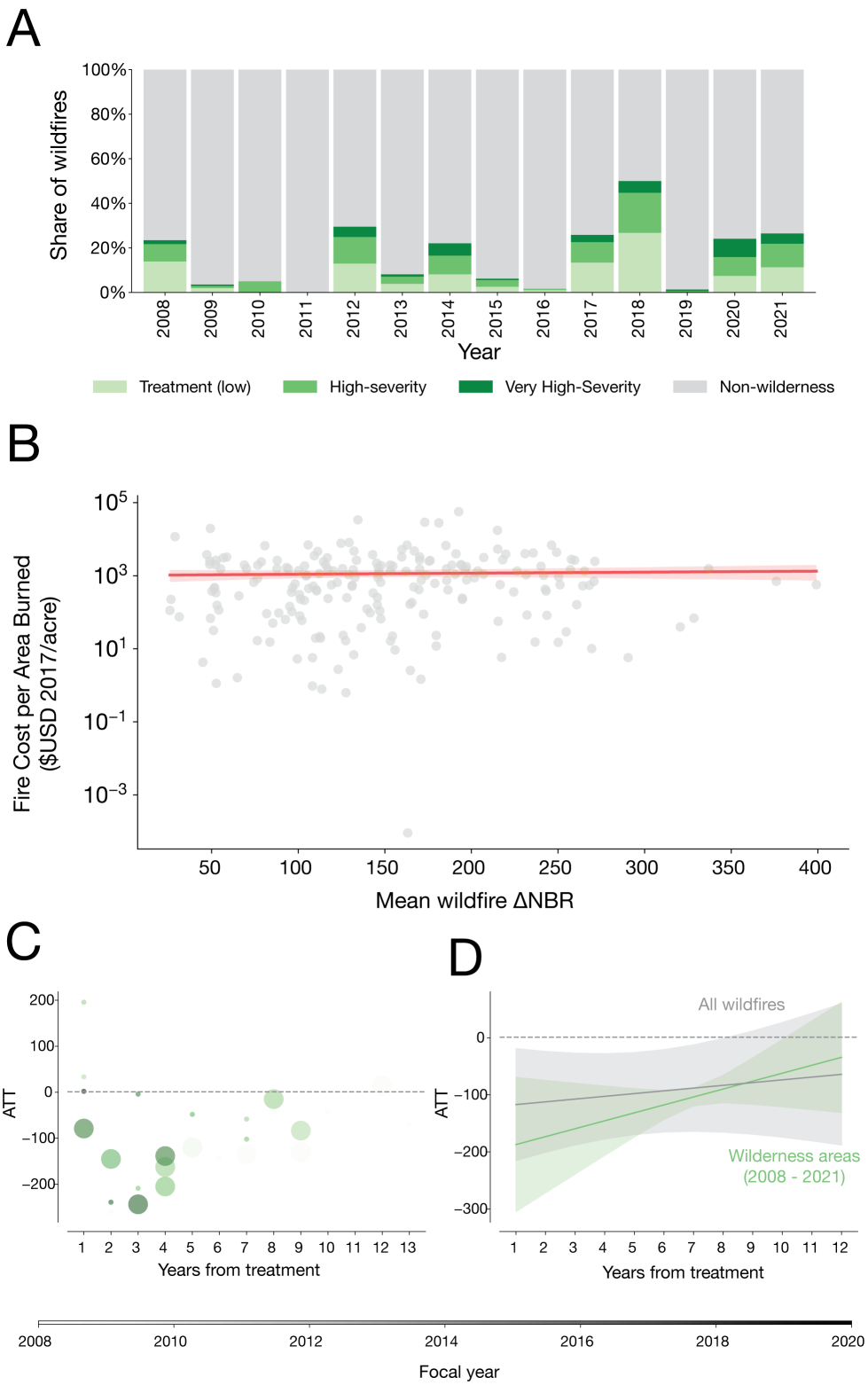

Figure S16: Role of fire suppression in treatment effect estimates. **a.** Restricting study sample to wilderness areas, where suppression efforts are often lower, offers an opportunity to study the role of suppression in treatment effect estimates, but most fires occur outside wilderness areas and some years have no low-severity treatments. **b.** Fire suppression costs per acre (from from [8]) do not vary by average burn severity of each fire. **c-d.** Low-severity treatments reduce the future fire severity in wilderness areas. As in Fig S11, left panel shows individual focal-year estimates of the ATT, and right panel shows pooled OLS fits to the individual data; green line is pooled estimate for wilderness areas, black line is the full-sample estimate for comparison.

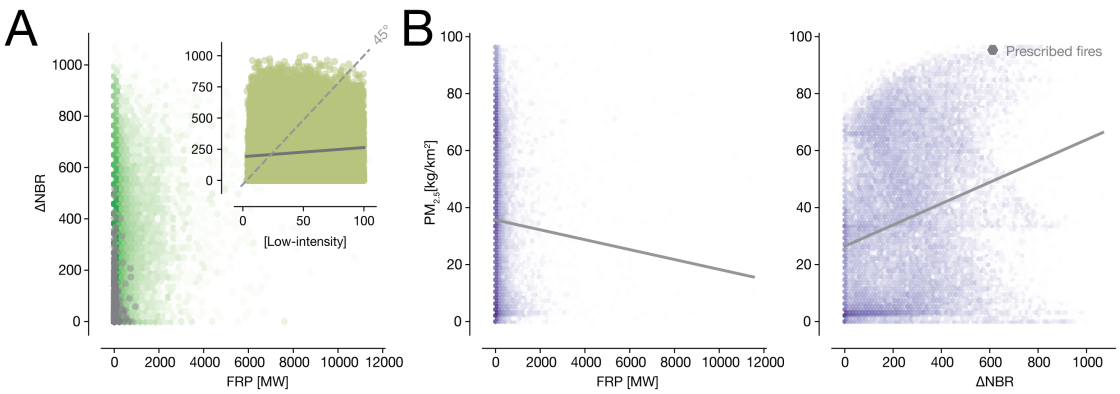

Figure S17: Fire Severity and fire intensity and their relationship with emissions. Using fire intensity data -Fire Radiative Power (FRP)- from MODIS derived measurements (`MOD09GA`) and `MYD09GA` and fire severity (ΔNBR) data from the Landsat 2 collection for all fires in the MTBS wildfire and prescribed fires dataset. **a.** shows the raw relationship between severity and intensity. The inset zooms over the low-intensity (0 - 100 MW) and shows that many low-intensity pixels have all severity classes, including very high-severity (¿500 ΔNBR). **b.** Using FINN [26], an emissions inventory dataset, we show that intensity and severity are not necessarily equally correlated to emissions from wildfires.

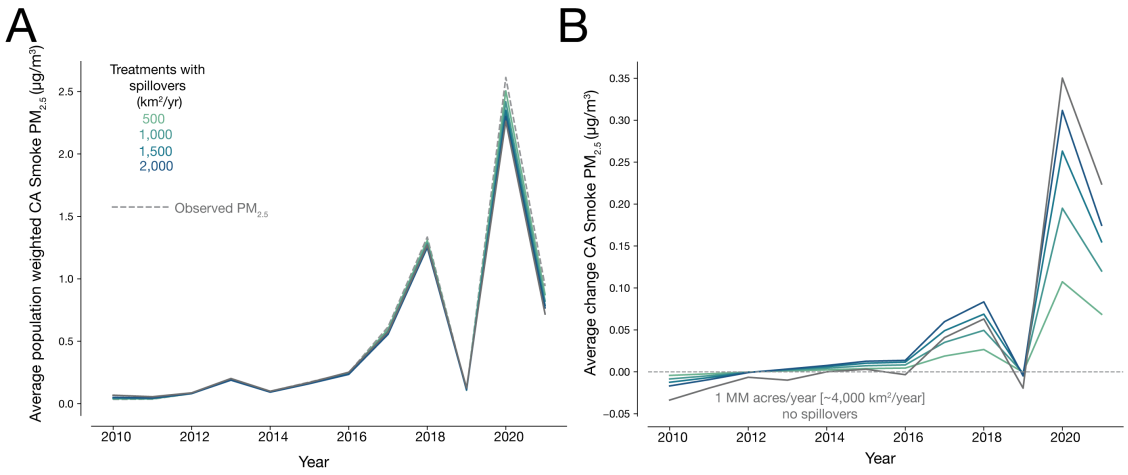

Figure S18: Average Smoke $PM_{2.5}$ concentration changes in CA as a result of simulated prescribed burning policies. **a.** Average population-weighted smoke $PM_{2.5}$ concentrations for the state under the simulated policies and the observed concentrations (dashed line) using data from [11]. Following estimates in [25] we assume that 88% of CA smoke concentrations originate from fires in CA, meaning that a prescribed burning policy in CA can only affect this proportion of smoke that originates from withing the state. **b.** Average reduction in smoke $PM_{2.5}$ concentrations from the different simulated policies, relative to observed smoke.

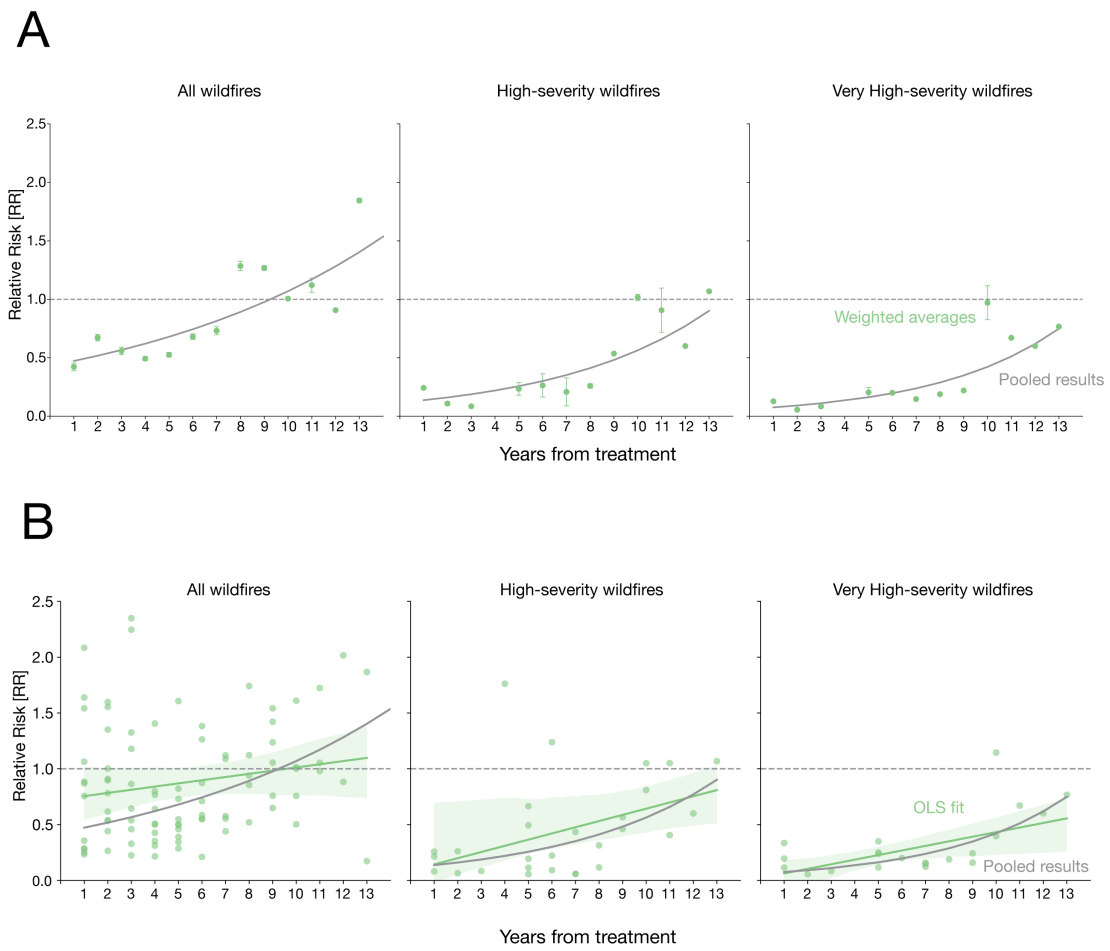

Figure S19: Protective effect of low-severity fires with alternate pooling. **a.** We pool the individual $\widehat{RR}$ estimates and lag using a weighted average. We include the original log-linear pooling from our main results (see Fig 2 in the manuscript) in gray for comparison. **b**. Protective effect of low-severity fires with a linear pooling, fit with OLS with no weighting, again compared with our main log-linear estimate. For visualization purposes we remove $\widehat{RR} > 2$, but they are included in our pooling regression.

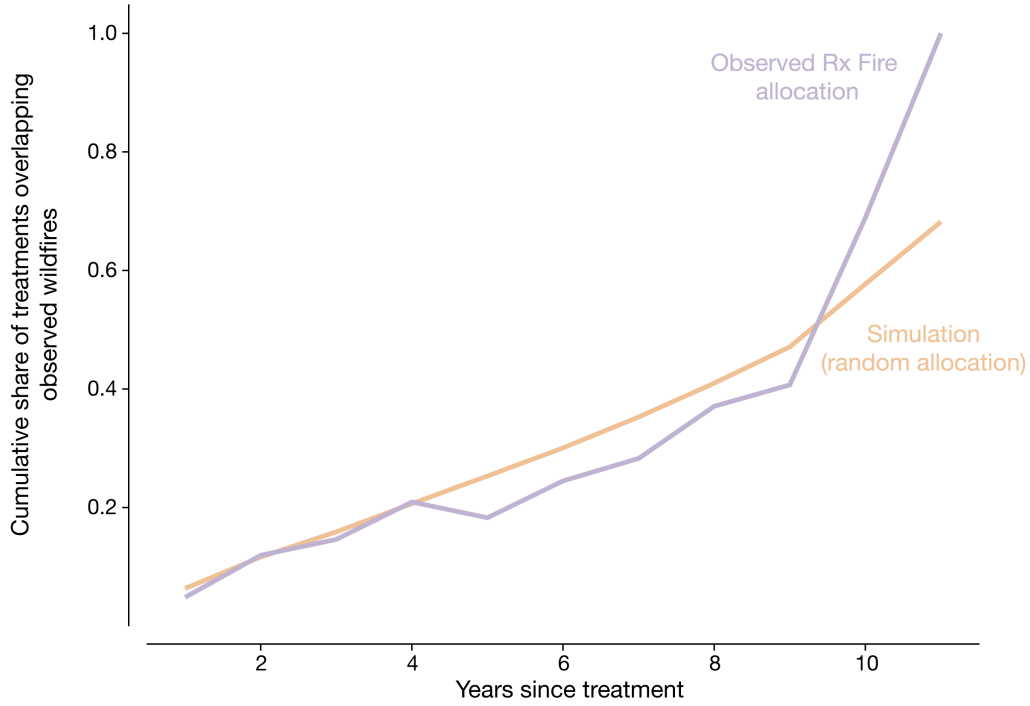

Figure S20: Targeting of simulated and observed prescribed fire policy. We calculate the policy targeting for both the simulated and observed prescribe fire policies as the average cumulative share of treatment area across all treatment years that overlaps with areas identified as wildfires in the MTBS dataset. The observed prescribed fire policy is taken from all broadcast prescribed fires in the CalFIRE FIRMS dataset (2010 - 2021) and shows how random simulations approximate the observed treatment targeting.

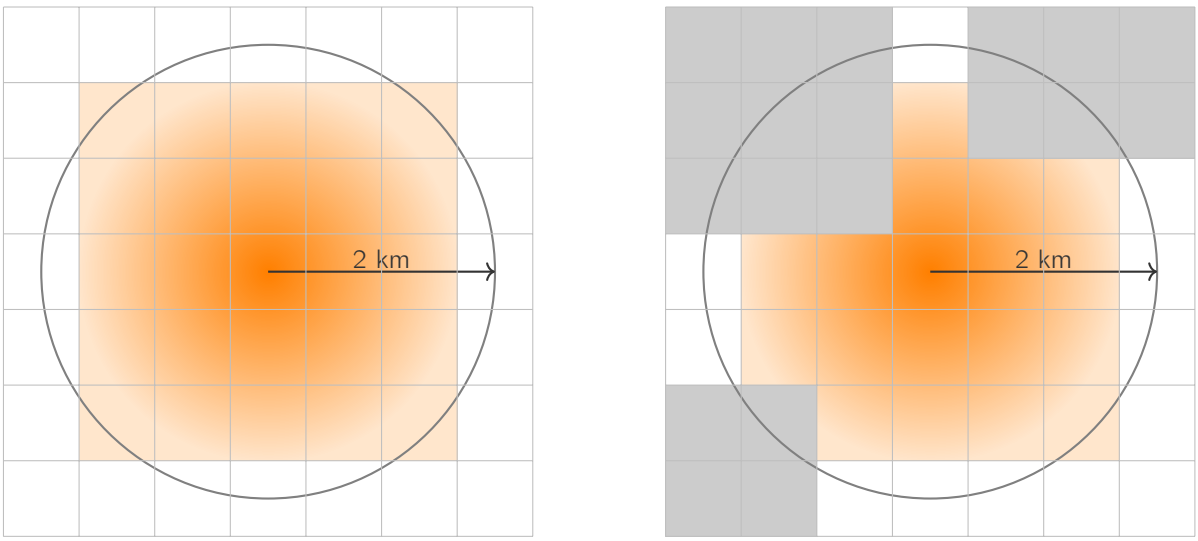

(a) Complete spillovers ($S_i = 24$)

(b) Incomplete spillovers ($S_i = 17$)

Figure S21: Simulating spillovers in simulations: To define spillovers in our simulations, we draw a 2 km^2 buffer around the treated pixel (dark orange) only including the neighboring pixels whose centroid is inside the buffer. When all neighboring pixels have not been treated, the spillover area is 24 km^2 as shown in (a). Since in our simulations we do not apply treatments in areas previously treated, we often have incomplete spillover areas (as shown in (b)) as previously treated pixels are removed from the spillover and then spillover areas are smaller than the optimal 25 km^2. This explains why often we have a diminishing number of treatments when we increase the number of treated areas with spillovers (Fig S13).

Supplemental Tables

Parameter	Description
$\beta_{i,\tau}^{\Delta NBR}$, $\delta_{i,\tau}^{\Delta NBR}$	From the estimates in the first section of the paper, we calculate the change in severity in period τ given the exposure to a treatment in the year of exposure ($\tau = 0$) for an specific vegetation-type pixel $i \in S$ (Fig S11) Additionally, we also estimate the spillover effects ($\delta^{\Delta NBR}$) for a given treatment. These last ones do not vary by vegetation type.
n_{τ}^{f}	The number of exposed pixels to fire in the year of exposure τ from the MTBS dataset.
$f_{PM_{2.5}}$	The relationship between fire-attributed smoke $PM_2.5$ concentrations ($\mu g/m^3$), integrated over time and space, and fire-specific summed severity.
Rx	The number of pixels we expose to Rx treatment.
$\underline{\Delta NBR}$	The average treatment severity from prescribed fire treatments. Following our MTBS data we estimate this is $\Delta NBR \approx 90$).
$\mathbb{P}(F)_{\tau}$	The observed probability that an arbitrary pixel in California burns in wildfire in any given year.

Table S1: Simulation parameters: Parameters used to estimate our prescribed fire policy simulations.

References

[1] Alberto Abadie, Alexis Diamond, and Jens Hainmueller. "Comparative Politics and the Synthetic Control Method". en. In: *American Journal of Political Science* 59.2 (Feb. 2015), pp. 495–510. ISSN: 00925853. DOI: 10.1111/ajps.12116.

[2] Alberto Abadie, Alexis Diamond, and Jens Hainmueller. "Synthetic Control Methods for Comparative Case Studies: Estimating the Effect of California's Tobacco Control Program". In: *Journal of the American Statistical Association* 105.490 (June 2010), pp. 493–505. ISSN: 0162-1459. DOI: 10.1198/jasa.2009.ap08746.

[3] Alberto Abadie and Javier Gardeazabal. "The Economic Costs of Conflict: A Case Study of the Basque Country". en. In: *American Economic Review* 93.1 (Mar. 2003), pp. 113–132. ISSN: 0002-8282. DOI: 10.1257/000282803321455188.

[4] Giuseppe Amatulli et al. "A suite of global, cross-scale topographic variables for environmental and biodiversity modeling". en. In: *Scientific Data* 5.1 (Mar. 2018), p. 180040. ISSN: 2052-4463. DOI: 10.1038/sdata.2018.40.

[5] Dmitry Arkhangelsky and Guido Imbens. "Causal models for longitudinal and panel data: a survey". In: *The Econometrics Journal* 27.3 (Sept. 2024), pp. C1–C61. ISSN: 1368-4221. DOI: 10.1093/ectj/utae014.

[6] Dmitry Arkhangelsky et al. "Synthetic Difference-in-Differences". en. In: *American Economic Review* 111.12 (Dec. 2021), pp. 4088–4118. ISSN: 0002-8282. DOI: 10.1257/aer.20190159.

[7] Susan Athey and Guido W. Imbens. "The State of Applied Econometrics: Causality and Policy Evaluation". en. In: *Journal of Economic Perspectives* 31.2 (May 2017), pp. 3–32. ISSN: 0895-3309. DOI: 10.1257/jep.31.2.3.

[8] Patrick Baylis and Judson Boomhower. "The Economic Incidence of Wildfire Suppression in the United States". en. In: *American Economic Journal: Applied Economics* 15.1 (Jan. 2023), pp. 442–473. ISSN: 1945-7782. DOI: 10.1257/app.20200662.

[9] Janet Bouttell et al. "Synthetic control methodology as a tool for evaluating population-level health interventions". en. In: *J Epidemiol Community Health* 72.8 (Aug. 2018), pp. 673–678. ISSN: 0143-005X, 1470-2738. DOI: 10.1136/jech-2017-210106.

[10] Center For International Earth Science Information Network (CIESIN). *Gridded Population of the World, Version 4 (GPWv4): Population Density Adjusted to Match 2015 Revision UN WPP Country Totals, Revision 11*. 2018. DOI: 10.7927/H4F47M65.

[11] Marissa L. Childs et al. "Daily Local-Level Estimates of Ambient Wildfire Smoke PM2.5 for the Contiguous US". In: *Environmental Science & Technology* 56.19 (Oct. 2022), pp. 13607–13621. ISSN: 0013-936X. DOI: 10.1021/acs.est.2c02934.

[12] Christopher Daly et al. "Physiographically sensitive mapping of climatological temperature and precipitation across the conterminous United States". en. In: *International Journal of Climatology* 28.15 (2008), pp. 2031–2064. ISSN: 1097-0088. DOI: 10.1002/joc.1688.

[13] Jeff Eidenshink et al. "A Project for Monitoring Trends in Burn Severity". en. In: *Fire Ecology* 3.1 (June 2007), pp. 3–21. ISSN: 1933-9747. DOI: 10.4996/fireecology.0301003.

[14] Jon E. Keeley. "Fire intensity, fire severity and burn severity: a brief review and suggested usage". en. In: *International Journal of Wildland Fire* 18.1 (Feb. 2009), pp. 116–126. ISSN: 1448-5516, 1448-5516. DOI: 10.1071/WF07049.

[15] Carl H Key and Nathan C Benson. "Landscape Assessment (LA)". en. In: (2006).

[16] Sean A. Parks et al. "Mean Composite Fire Severity Metrics Computed with Google Earth Engine Offer Improved Accuracy and Expanded Mapping Potential". en. In: *Remote Sensing* 10.6 (June 2018), p. 879. ISSN: 2072-4292. DOI: 10.3390/rs10060879.

[17] Sean A. Parks et al. "Previous Fires Moderate Burn Severity of Subsequent Wildland Fires in Two Large Western US Wilderness Areas". en. In: *Ecosystems* 17.1 (Jan. 2014), pp. 29–42. ISSN: 1432-9840, 1435-0629. DOI: 10.1007/s10021-013-9704-x.

[18] Krishna Rao et al. "Plant-water sensitivity regulates wildfire vulnerability". en. In: *Nature Ecology & Evolution* 6.3 (Mar. 2022), pp. 332–339. ISSN: 2397-334X. DOI: 10.1038/s41559-021-01654-2.

[19] Sarah A Reifeis and Michael G Hudgens. "On Variance of the Treatment Effect in the Treated When Estimated by Inverse Probability Weighting". In: *American Journal of Epidemiology* 191.6 (May 2022), pp. 1092–1097. ISSN: 0002-9262. DOI: 10.1093/aje/kwac014.

[20] Donald Rubin. "Estimating Causal Effects of Treatments in Experimental and Observational Studies". en. In: *ETS Research Bulletin Series* 1972.2 (1972), pp. i–31. ISSN: 2333-8504. DOI: 10.1002/j.2333-8504.1972.tb00631.x.

[21] Daniel L. Swain et al. "Climate change is narrowing and shifting prescribed fire windows in western United States". en. In: *Communications Earth & Environment* 4.1 (Oct. 2023), pp. 1–14. ISSN: 2662-4435. DOI: 10.1038/s43247-023-00993-1.

[22] Daniel L. Swain et al. "Hydroclimate volatility on a warming Earth". en. In: *Nature Reviews Earth & Environment* 6.1 (Jan. 2025), pp. 35–50. ISSN: 2662-138X. DOI: 10.1038/s43017-024-00624-z.

[23] Jonathan Wang. *Fractional vegetation cover in California, 1985 - 2023*. en. Nov. 2024. DOI: 10.7910/DVN/KMBYYM.

[24] Jonathan A. Wang et al. "Losses of Tree Cover in California Driven by Increasing Fire Disturbance and Climate Stress". en. In: *AGU Advances* 3.4 (2022), e2021AV000654. ISSN: 2576-604X. DOI: 10.1029/2021AV000654.

[25] Jeff Wen et al. "Quantifying fire-specific smoke exposure and health impacts". In: *Proceedings of the National Academy of Sciences* 120.51 (Dec. 2023), e2309325120. DOI: 10.1073/pnas.2309325120.

[26] Christine Wiedinmyer et al. "The Fire Inventory from NCAR version 2.5: an updated global fire emissions model for climate and chemistry applications". English. In: *Geoscientific Model Development* 16.13 (July 2023), pp. 3873–3891. ISSN: 1991-959X. DOI: 10.5194/gmd-16-3873-2023.

[27] Xiao Wu et al. "Low-intensity fires mitigate the risk of high-intensity wildfires in California's forests". In: *Science Advances* 9.45 (Nov. 2023), eadi4123. DOI: 10.1126/sciadv.adi4123.

[28] Qingyuan Zhao. "Covariate balancing propensity score by tailored loss functions". In: *The Annals of Statistics* 47.2 (Apr. 2019), pp. 965–993. ISSN: 0090-5364, 2168-8966. DOI: 10.1214/18-AOS1698.

[29] José R. Zubizarreta. "Stable Weights that Balance Covariates for Estimation With Incomplete Outcome Data". In: *Journal of the American Statistical Association* 110.511 (July 2015), pp. 910–922. ISSN: 0162-1459. DOI: 10.1080/01621459.2015.1023805.